Impact of advanced wind power ancillary services on power system

Hansen, Anca Daniela; Altin, Müfit

Publication date:
2015

Document Version
Publisher's PDF, also known as Version of record

Impact of advanced wind power ancillary services on power system

DTU Vindenergi
E Rapport 2015

Anca D. Hansen and Müfit Altin

DTU Wind Energy E-0081

January 2015

DTU Vindenergi
Institut for Vindenergi

Forfatter(e): Anca D. Hansen, Müfit Altin
Titel: Impact of advanced wind power ancillary services on power system
Institut: DTU Wind Energy

Resume (mask. 2000 char.):

The objective of this report is to illustrate and analyse, by means of simulation test cases, the impact of wind power advanced ancillary services, like inertial response (IR), power oscillation damping (POD) and synchronising power (SP) on the power system. Generic models for wind turbine, wind power plant and power system are used in the investigation.

2015

ISBN 978-87-93278-26-4

Kontrakt nr.:
[Tekst]

Projektnr.:
[Tekst]

Sponsorship:
PSO

Forside:
[Tekst]

Danmarks Tekniske Universitet
DTU Vindenergi
Nils Koppels Allé
Bygning 403
2800 Kgs. Lyngby
Telefon

www.vindenergi.dtu.dk

Table of Contents

Abbreviations

CPP	conventional power plants
IR	inertial response
PCC	point of common coupling
POD	power oscillation damping
PoM	point of measurement
pu	per-unit
ROC	rate-of-change
SP	synchronizing power
WPP	wind power plant
WPPC	wind power plant controller
WTG	wind turbine

Preface

This report is elaborated as part of the work done in the project titled “Enhance ancillary services from wind power” (EaseWind). The project was funded by the Danish TSO as PSO project 2011 no. 10653, and it was carried out in collaboration between Vestas Wind System A/S, DTU Wind Energy, DTU Compute and Aalborg University IET. Vestas Wind System A/S has been the manager of the project. The report has been internally reviewed and approved by Vestas and Aalborg University IET.

1 Introduction

1.1 Scope of the document

The scope of this document is to illustrate and analyse, by means of simulation test cases, the impact of wind power advanced ancillary services, like inertial response (IR), power oscillation damping (POD) and synchronising power (SP) on the power system.

The simulation test cases are designed for reproducing the respective ancillary service and a realistic behaviour and operation of medium/large power systems with high wind power penetration. In this investigation, as a limitation of the scope, an independent actuation of the new ancillary services is considered, namely no multiple ancillary service algorithms are running in parallel. The impact of each individual ancillary service on the power system is presented for different wind power penetration levels. The technical capability of the wind power plants to deliver the new advanced ancillary services is illustrated and discussed through simulations. Details for the developed wind turbine and wind power plant models are in [1-3]. The verification of the models is out of scope of the document. The present report is not targeting to show the tuning methodology of the controller parameters, as these parameters are tuned in the work done in WP1 of the project. Furthermore, the communication delays are not included in the implementation of the controllers, as they are assumed compensated based on the information delivered in the work done in WP1.

1.2 Reading guidelines

The reader is assumed to be familiar with the modelling and control capabilities of modern WPP, as well as with stability mechanisms and controls in power systems.

1.3 References

[1] A. Hansen and M. Altin, “Modelling of wind power plant controller, wind speed time series, aggregation and sample results”, DTU Wind Energy E-0064, 2015

[2] P. Mahat,”Power system Model for New ancillary services”, Report Aalborg University, 2013

[3] Müfit A., “Dynamic Frequency Response of Wind Power Plants”, PhD Thesis, Aalborg University, Aalborg, Denmark, 2012.

[4] Adamczyk, A., “Damping of Low Frequency Power System Oscillations with Wind

Power Plants", PhD Thesis, Aalborg University, Aalborg, Denmark, 2012.

2 Enhanced ancillary services from wind power

In order to assess the impact of wind power advanced ancillary services, like inertial response (IR), power oscillation damping (POD) and synchronising power (SP) on the power system, the generic power system described in [2] with different wind power penetration scenarios, and the aggregated WPP model, described in [1], are utilised.

Figure 1 depicts a typical configuration and control architecture of a WPP. It consists of a WPP, composed of several wind turbines connected to the grid at the PCC through a main transformer, a wind power plant controller WPPC, communication system and measurement devices for voltage, current, grid frequency and power at the PCC. The WPPC is getting power settings from TSO via SCADA system. Besides a dispatch block, ancillary services block and services allocation block, the WPPC also contains a grid condition and monitoring block, which delivers the grid frequency and frequency gradient estimation, active and reactive power calculation based on voltage and currents measurements.

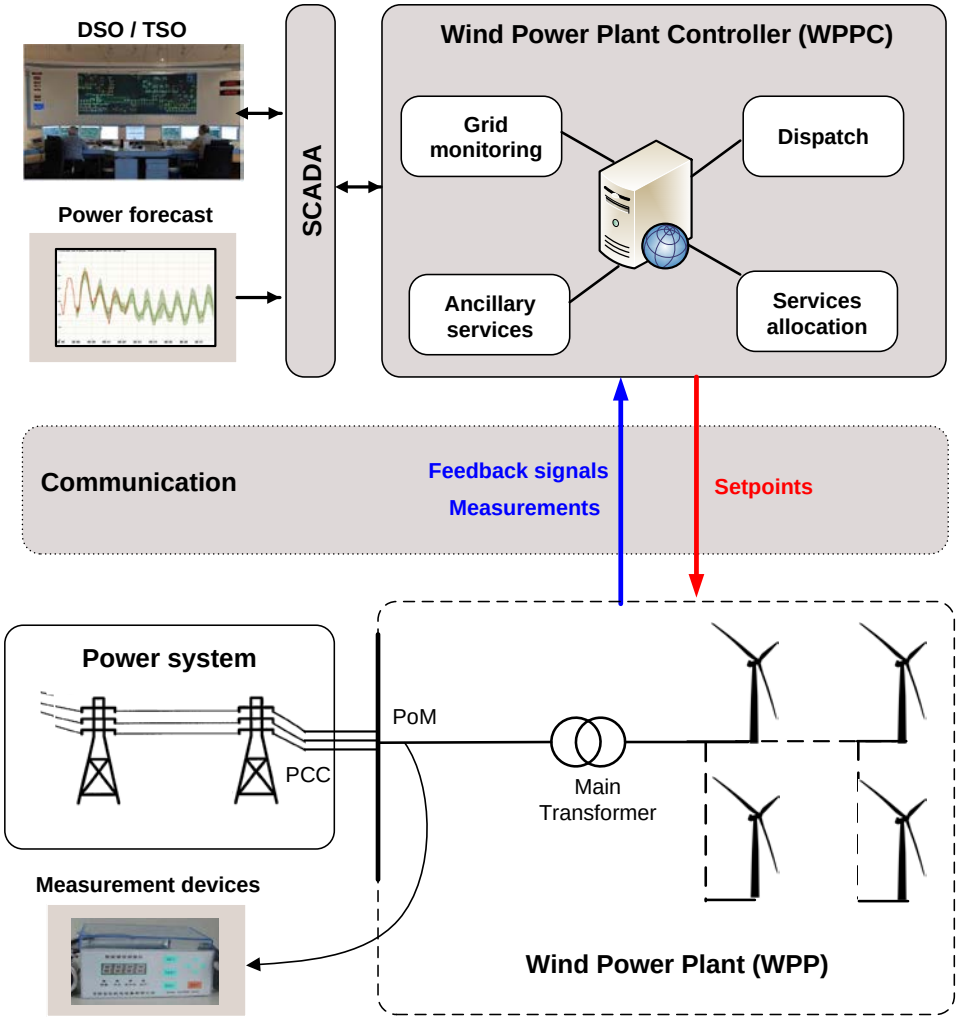

Figure 1: Wind power plant configuration.

The overall structure for the Wind Power Plant Controller (PPC), described in details in [1] is given in Figure 2. It consists of an ancillary services (control functionalities) block, services allocation block and a dispatching block.

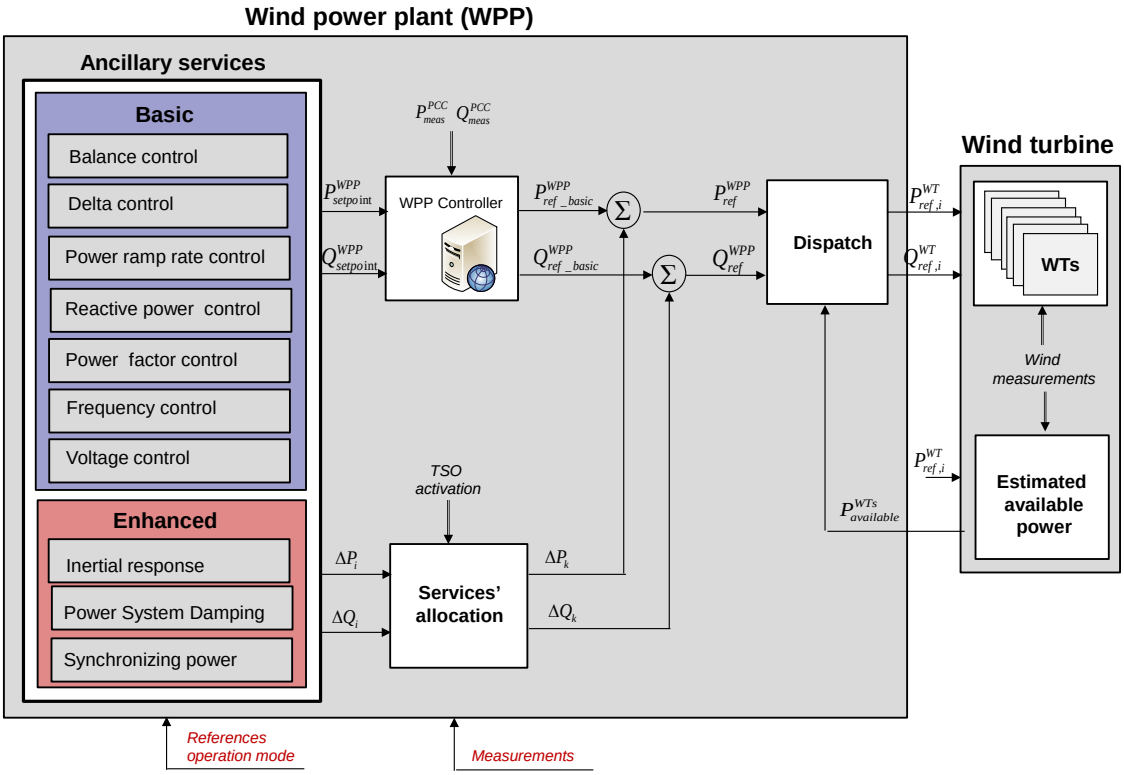

Figure 2: Wind power plant control architecture [1].

The new control functionalities, targeted in EASE Wind project, are:

- inertial response (IR),
- synchronising power (SP)
- power oscillation damping (POD)

on the power system to the power system with large wind power penetration.

Figure 3 depicts the typical in/out waveforms for the new control functionalities implemented in the WPP level together with the default WPPC controls [1]. The test cases, presented in this report, will consider one activated control functionality per time at the related power system events. As described in [1], an aggregated wind power plant model is used to represent the generic behaviour of the wind power plant with the stability phenomena needed amount of detail. Accordingly, the wind power plant is assumed as a single unit, thus the dispatch block distributing references for individual wind turbines inside WPP is omitted in this study.

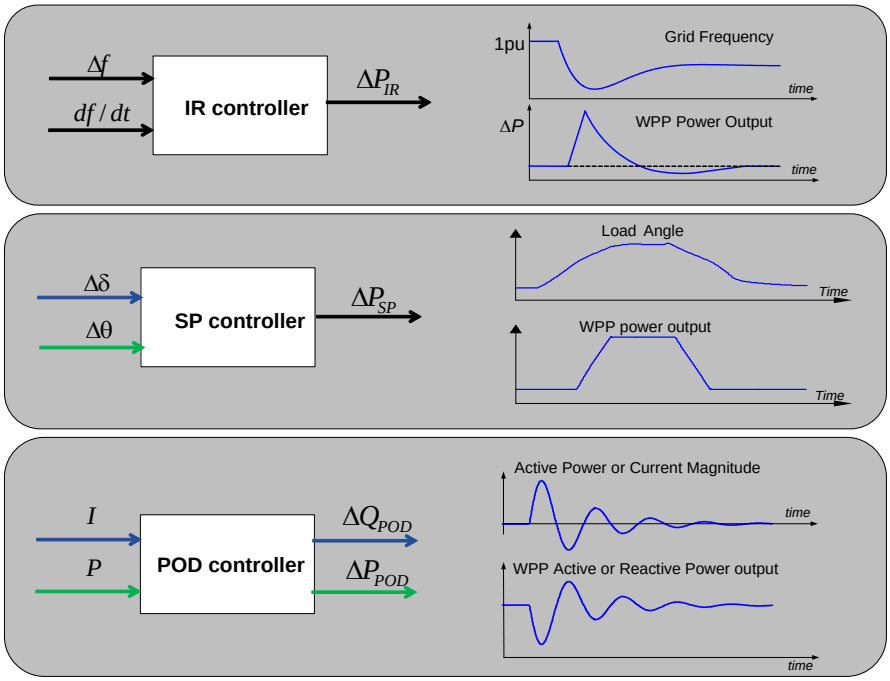

Figure 3: Typical in/out waveforms overview of the new control functionalities [1].

The aggregated WPP model is integrated in the 12-bus power system model [2] in order to perform and analyse different simulation test cases. The generic power system model, shown in Figure 4, has been developed with the wind power scenarios which vary from 0% to 50% penetration levels. It reproduces the necessary grid characteristics for actuation and impact assessment of the new enhanced ancillary services, like inertial response (IR), power oscillation damping (POD) and synchronising power (SP) on the power system. A complete description of it can be

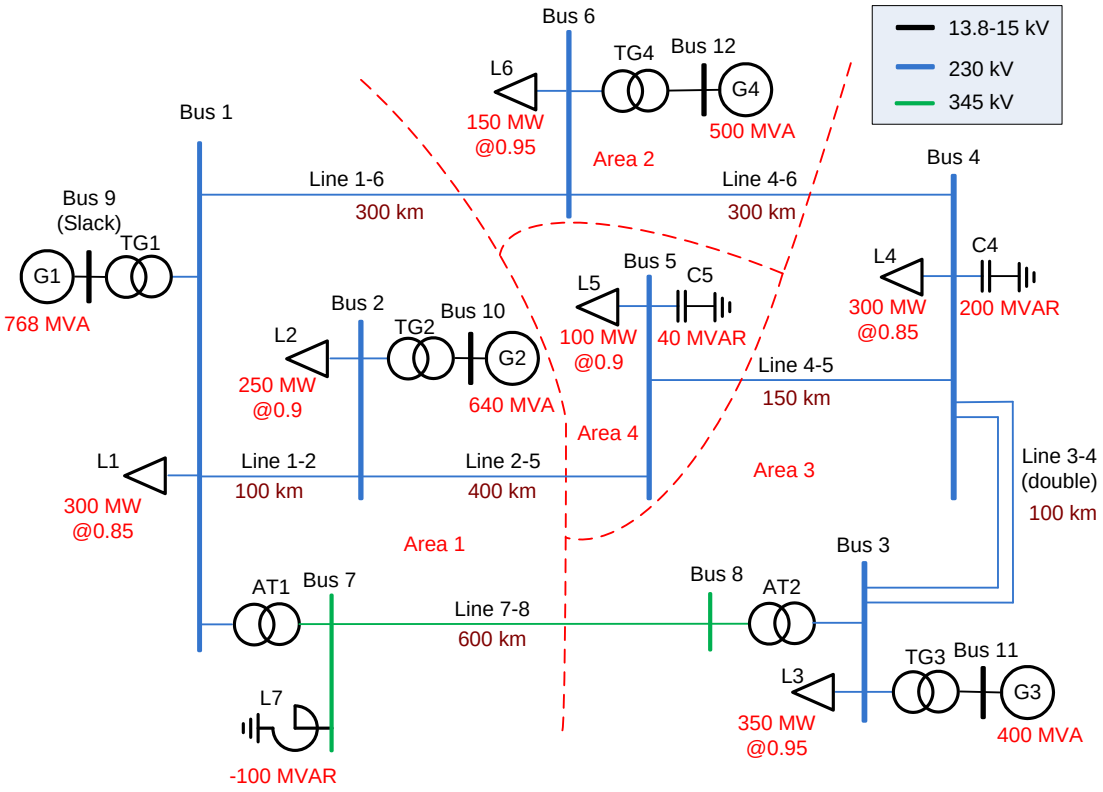

Figure 4: Structure for Generic 12-bus System for Wind Integration Studies [2].

found in [2].

3 Test cases

The grid disturbance events and their impact on the power system for each new ancillary service in focus are indicated in Table 1.

Ancillary Services	Event	Focus on Power System
IR	**Loss of the largest generating unit (N-1 criteria)** *(Tripping of two generation units from G2, i.e. 200MW generation loss)*	**Large frequency excursion**
POD	**Short circuit event** *(Temporary high impedance symmetric fault at busbar 6)*	**Electromechanical oscillations**
SP	**Load increase event** *(Load in Bus 4 is ramped up-down 25% and 50%, during five seconds each case)*	**Voltage/Rotor angle variations**

Table 1:Grid disturbance events for IR, POD and SP.

Only one of the ancillary service functionalities, indicated in Table 1, is selected during one event by the service allocation block illustrated in Figure 2. This means that even though all the ancillary services controllers are active in parallel, only the output of one of them is selected by the allocation block and used further to adjust the power references to the WPP.

The following different instantaneous wind penetration cases, based on 12-bus power system model [2], are in focus to study the new ancillary services:

- 0% online wind power penetration – no WPP (Base Case)
- 20% online wind power penetration – WPP at bus 5
- 50% online wind power penetration – WPP1 at Bus 5, WPP2 at Bus 3 and WPP3 at Bus 4[1].

The *online wind power penetration* represents the amount of the load demand which is provided by online wind power[2]. At the 20% instantaneous wind penetration, the conventional generator size is kept constant while wind power and loads are increased. At the 50% instantaneous wind power penetration, conventional units are decommissioned while the load demand is kept at 20% penetration level. This is summarized in Table 2:

1 The nominal power of WPP1 connected at bus5 is 400MW, of WPP2 connected at bus3 is 200MW and of WPP3 connected at bus4 is 250MW.

2 For example, a 20% online wind power penetration in a power system with a given amount of consumers means that 20% of the power used by the consumers is coming from wind power plants, while the rest from conventional power plants.

Cases	0%	20%	50%
CPP (GW)	2.00	2.00	1.65
Load (GW)	1.45	1.85	1.85
WPP (GW)	0.00	0.40	1.00

Table 2: Wind power penetration scenarios.

The power system response in the Base Case (voltages, currents, powers) is taken as baseline for power system security and stability assessment. The effect of the wind power controls for the different instantaneous wind penetrations is compared to this Base Case.

The simulations are performed allowing 10% curtailment for wind turbines. Two different wind speed levels corresponding to partial load and full load, respectively, are considered for IR and SP:

- 0.69 pu power (0.86 pu wind speed)
- 1.00 pu power (1.2 pu wind speed)

4 Inertial Response (IR)

In the simulations, the largest infeed from G2 is tripped to demonstrate the performance of the inertial response control for the 20% and 50% wind power penetration scenarios compared to the basic case. There is enough reserve in the system to recover the frequency above the load shedding limit.

The need for inertial response control is depicted in Figure 5 by the system frequency measured at the generator G1 following the largest generation loss (i.e. 200MW) at time = 0sec for the different wind power penetrations indicated in Table 2.

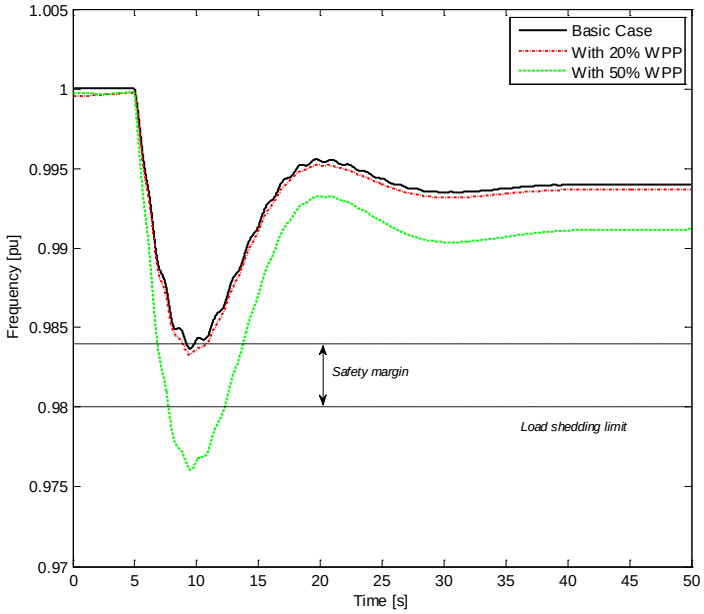

Figure 5: System frequency excursion following the largest generation loss (i.e. 200MW) for different wind power penetrations.

As it is seen in Figure 5, the loss of the generation may lead to some load shedding as the frequency hits the load shedding limit. Notice that the frequency excursion increases with the increase in wind power penetration. For the power system considered in the present investigation, it is revealed that for wind power penetration levels higher than 20% the minimum frequency point even reaches lower values exceeding the trip limit of load shedding relays.

This is a typical example for showing a decrease in the system inertia while decommissioning conventional generator units in order to accommodate more wind power. In order to avoid the load shedding, wind power should provide additional power equivalent to the inertial response of the synchronous generators.

4.1 Simulation test cases for IR

The simulation test cases proposed for assessing IR impact on the power system are illustrated Table 3.

PoM	Input signal	Output signal	% wind	Event	Ctrl. Param.	TC_IR$_i$ no.	IR Case
-	-	-	0%	200MW loss from G2 (Bus 10)	-	TC_IR$_0$	0
Bus 5	F & ROCOF	ΔP_{IR}	20%	200MW loss from G2 (Bus 10)	IR-P1	TC_IR$_1$	1
Bus 5 Bus 4 Bus 3	F & ROCOF	ΔP_{IR}	50%	200MW loss from G2 (Bus 10)	IR-P2	TC_IR$_2$	2

Table 3: Simulation test cases for IR.

4.2 Success Criteria

The IR functionality aims to provide the WPP with the following characteristics:

- WPPs with IR contribute to dynamic temporary grid frequency stabilization during large power imbalances in the system.
- IR control effort is within the wind turbine's capabilities.

Besides these overall success criteria, the effectiveness of IR functionality is evaluated based on the following success criteria:

Characterization	Specifications	Identifier
Nadir	Grid frequency deviation (nadir) is inside allowed limits. In this case, above 49.2 Hz (0.984pu) for the largest generation loss.	IR-SC-01
ROCOF	Maximum ROCOF at a given post-event time is lower than relay settings from Grid Code. In this case 0.4 Hz/s at 200ms after event.	IR-SC-02
Stability	The action of IR functionality is not worsening the system oscillations amplitude and damping ratio, compared to the no-wind penetration case. A "double dip" in the grid frequency (e.g. due to WTG recovery) shall not be crated.	IR-SC-03

Table 4: Success criteria for IR.

The simulation results are shown in the following subsections assuming first that all the aggregated WPPs operate at partial load (i.e. 0.86pu wind speed) and then at full load (i.e. 1.2 pu wind speed).

4.3 Inertial response simulations – partial load case (0.86 pu wind speed)

Figure **6** illustrates the frequency excursion during the IR event defined in Table 1 both for the basic case (i.e. no wind power) and the case with 20% wind power online penetration with and without activation of IR ancillary service inside WPPs. Since the conventional power plants are not replaced in 20% wind power scenario, there is not considerable difference between the basic case (0% wind power) and 20% wind power scenario without IR contribution.

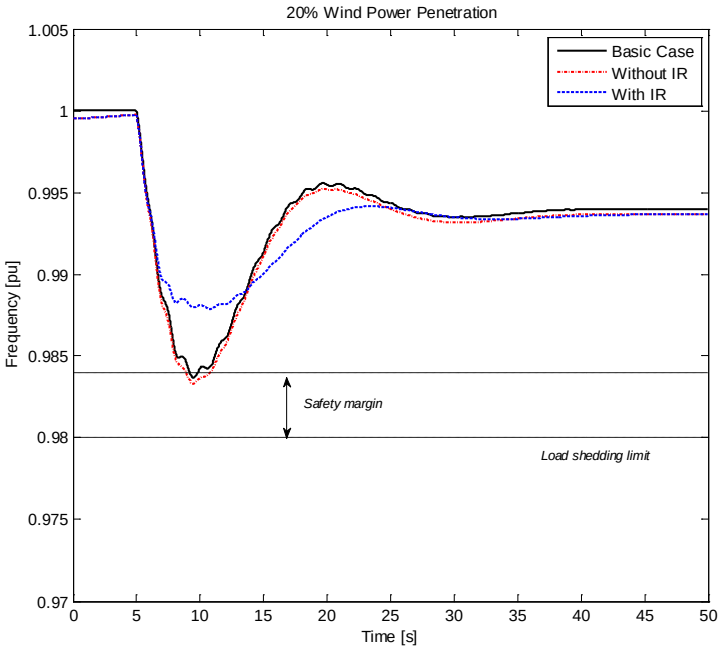

Figure 6: System frequency excursion during IR event, **0.86pu wind speed and** 20% wind power penetration with and without inertial response from WPPs.

Figure 7 compares the 50% wind power penetration case where no IR inside WPPs is activated with the cases where the IR is activated one by one first inside WPP1, then in WPP2 too and in the last also in WPP3 too.

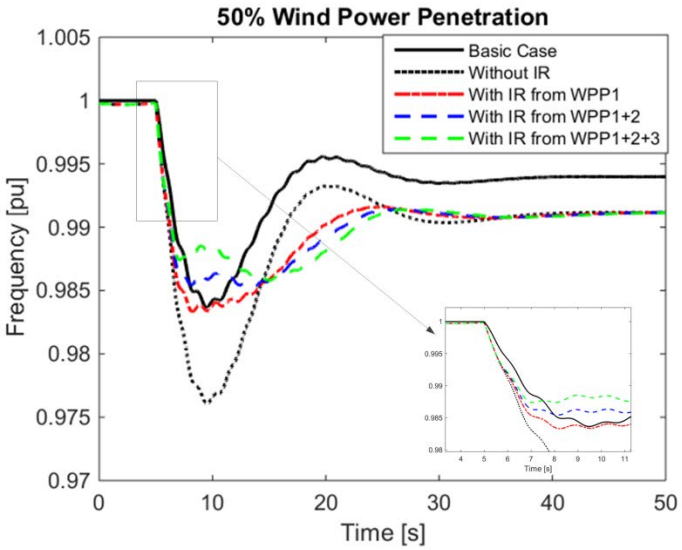

Figure 7: System frequency excursion during IR event at **0.86pu** wind speed and 50% wind power penetration with and without inertial response from WPPs.

The results illustrated in Figure **7** are consistent with the results depicted in Figure **5** , namely that the decommissioning of conventional generator units by accommodation of 50% wind power, decreases the system inertia and the nadir easily exceeds the allowed limits if no additional IR control is implemented inside WPPs. As shown in Figure **7**, the wind power improves the inertia of the system by providing additional power equivalent to the inertial response of the synchronous generators. Notice that, both the gradient of the frequency excursion and the nadir decrease, when all WPPs participate actively with IR. When all WPPs, namely WPP1, WPP2 and WPP3 are contributing with IR, the nadir is just above the load shedding limit.

According to the simulation results illustrated in **Figure 7** for the generic power system a double dip occurs in the system frequency when more than one WPP is contributing with IR. This situation is typically not preferred by power system operators. Only in Canada, Hydro-Quebec allows the WPPs to go to recovery period (up to 2min.) and accepts the second dip if it's not lower than the first dip. In the simulation case, there is no recovery period of the WTs, however injected active power from WPPs is large compared to the response time of the conventional power plants' governors. Further tuning of the parameters when all WPPs are required to contribute with IR and even coordination from TSOs of these contributions might be needed to avoid the double dip in the power system frequency.

The ROCOF results during IR event at 0.86pu wind speed are depicted in Figure **8** for all three cases: 0%, 20% and 50% wind power penetration. It can be noticed that the maximum ROCOF at 200ms after the fault event, i.e. the given post-event time as indicated in Table 4, is 0.25Hz/s, namely lower than the relay setting of 0.4Hz/s from grid codes.

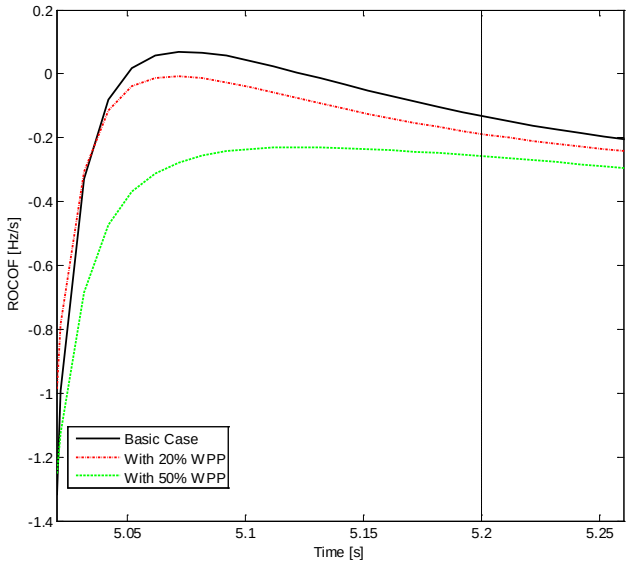

Figure 8: ROCOF during 200ms after the largest infeed loss

Figure **9** illustrates the system frequency measured at the generator G1, the electrical power generated by each WPP and their available power for for 0.86pu wind speed and 50% wind power penetration scenario. The curtailment of 0.1pu is visible. The available power has been implemented as described in [1]. It follows the gradient of the active power reference. It is worth mentioning that due to the dynamic estimation of the available power, depending on the power reference changing, and not only on the power curve, the wind turbine is not overloaded while it is contributing with IR. Notice that the electrical powers generated by all WPPs during the IR event are similar. The maximum of the inertial response contribution ΔP_{IR} of WPPs is 12% of the rated power.

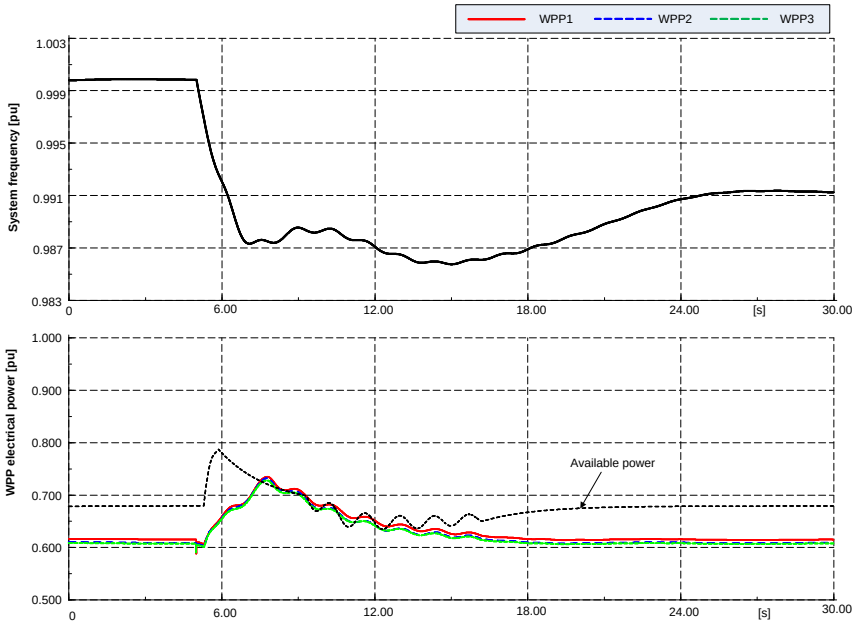

Figure 9: Frequency excursion, WPPs electrical power and ΔP_{IR} **of** WPPs during IR event – for **0.86pu wind speed** and 50% wind power penetration scenario.

Figure 10 depicts what is the impact of the inertia response action on the output of the other two services, namely POD and SP controllers. The figure shows thus the WPP inertial response, power oscillation damping and synchronous power contribution, i.e. ΔP_{IR}, ΔP_{POD} and ΔP_{SP} respectively, when only IR ancillary service is selected by the allocation services block, namely when only the output of the IR controller is further sent to WPP. Notice that IR contribution in 20% and 50% wind power penetration case are almost similar, though slightly higher for 50% case. The presence of light oscillations in the signals in the 50% case indicates that, as expected, the power system is slightly stronger in 20% case than 50% wind power penetration scenario. The IR response action has a very small influence on the active power output ΔP_{POD} of the POD. The variation of delta contribution signals ΔP_{POD} is smaller for 20% case. Notice that there is no any influence on the reactive power output ΔQ_{POD} of the POD controller and of the synchronising power output ΔP_{SP} of the SP controller.

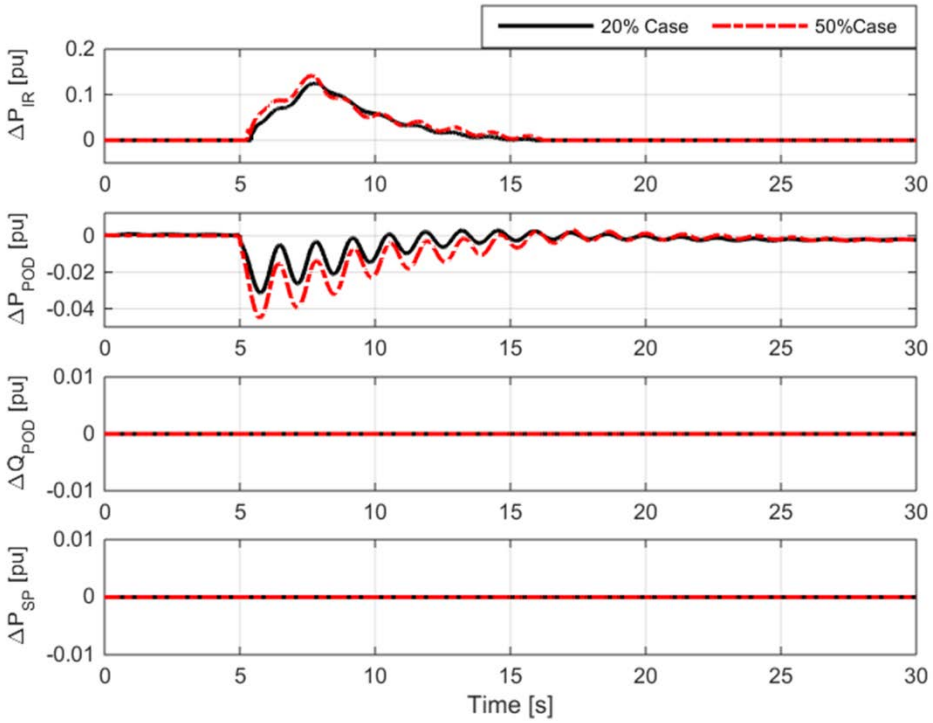

Figure 10: Contributions from WPP during IR event at **0.86pu wind speed** – for 20% and 50% wind power penetration scenarios.

Figure 11 illustrates the wind turbine performance during the grid frequency deviation, while the IR control functionality is activated in 50% wind power penetration scenarios at a low wind speed of 0.86pu. The figure illustrates the active power, rotational speed, pitch angle and shaft torque.

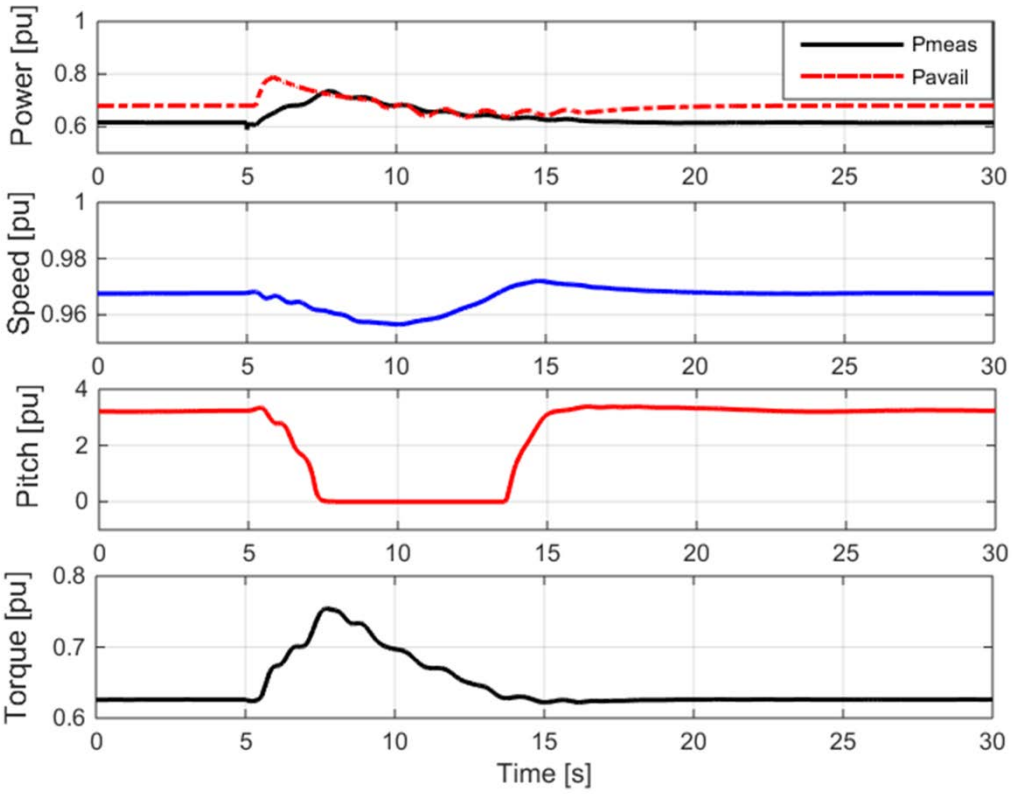

Figure 11: Wind turbine performance during IR event **at 0.86pu wind speed** – for 50% wind power penetration scenarios.

As also depicted in Figure 10, the wind turbine is not overloaded while it is supporting the grid with IR. As expected, the rotational speed is decreasing during IR contribution, however without reaching its acceptable minimum value. Notice that even the wind turbine is running at low wind speeds, where the pitch controller is typically inactive, in this simulation the pitch controller is active due to the fact that the turbine is running with 10% curtailment. However in the moment of IR event, the pitch angle drops to zero where it remains until IR contribution is finished. During IR contribution, wind turbines torque increases as result of decreasing the rotational speed.

4.4 Inertial response simulations – full load case (1.2 pu wind speed)

Figure 12 illustrates the frequency excursion during the IR event, defined in Table 1, illustrates both for the basic case (i.e. no wind power) and the 20% wind power online penetration case, during 1.2pu wind speed and with and without activation of IR ancillary service inside WPPs. The frequency excursion for 20% penetration for full load case is similar to that for partial load case is that illustrated in Figure **6**.

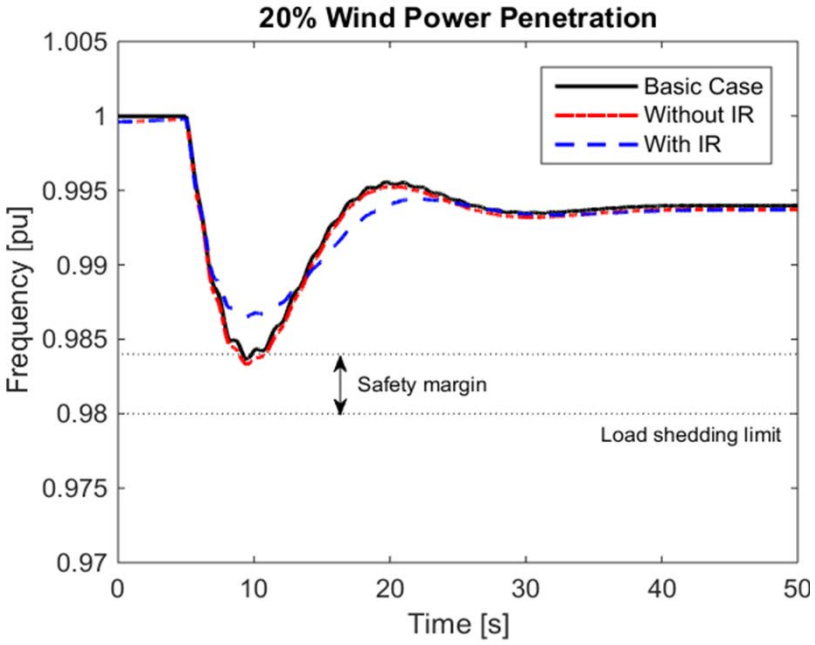

Figure 12: System frequency excursion during IR event, 1.2pu wind speed and 20% wind power penetration with and without inertial response from WPPs.

It is worth noticing that for the power system considered in this study, the frequency excursion during the loss of the largest generating is almost the same for the basic case and for 20% wind power penetration case without IR, not exceeding the load shedding limit. However, notice that the situation when WPP is contributing with IR is slightly better even than the basic case.

Figure 13 compares the 50% wind power penetration case where no IR inside WPPs is activated with the cases where the IR is activated one by one first inside WPP1, then in WPP2 too and in the last also in WPP3 too.

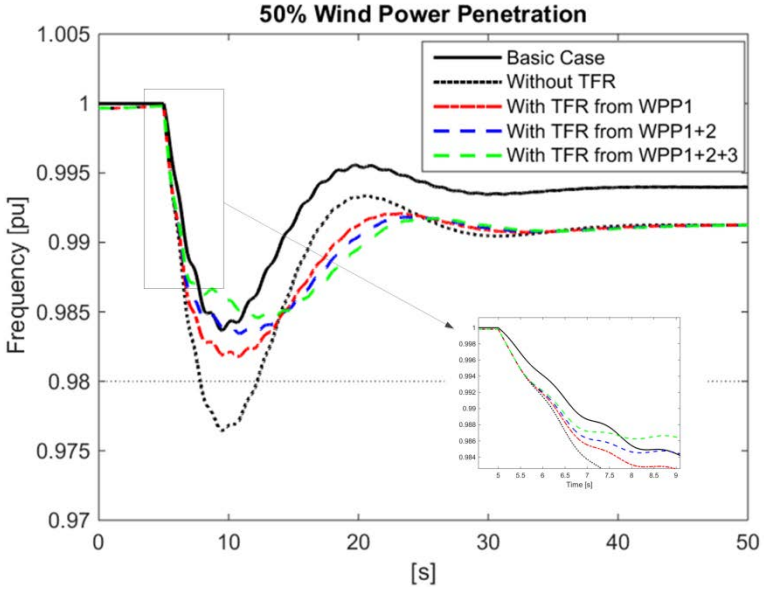

Figure 13: System frequency excursion during IR event, 1.2pu wind speed and 50% wind power penetration with and without inertial response from WPPs.

The results illustrated in Figure **13** are consistent with the results depicted in Figure 5, namely that the decommissioning of conventional generator units by accommodation of 50% wind power, decreases the system inertia and the nadir easily exceeds the allowed limits if no additional IR control is implemented inside WPPs. As shown in Figure **13**, the wind power improves the inertia of the system by providing additional power equivalent to the inertial response of the synchronous generators.

Both the gradient of the frequency excursion and the nadir decrease when all WPPs participate actively with IR. As expected, due to its double size compared with the rest of WPPs, WPP1's IR contribution to the power system is largest. However, as shown in Figure **13** , the IR contribution only from WPP1 is not enough to bring the nadir of the grid frequency excursion inside the allowed limits.

It is worth mentioning that, as illustrated in **Figure 13**, a double dip occurs in the system frequency also during IR event and 1.2pu wind speed when all WPPs are contributing with IR. This result shows that the IR contribution of WPPs should be coordinated by TSOs considering the activation time and gain of the controller.

The same ROCOF result, as illustrated in Figure **8** for 0.86 wind speed, is depicted in Figure **14** for 1.2pu wind speed and all three case: 0%, 20% and 50% wind power penetration.

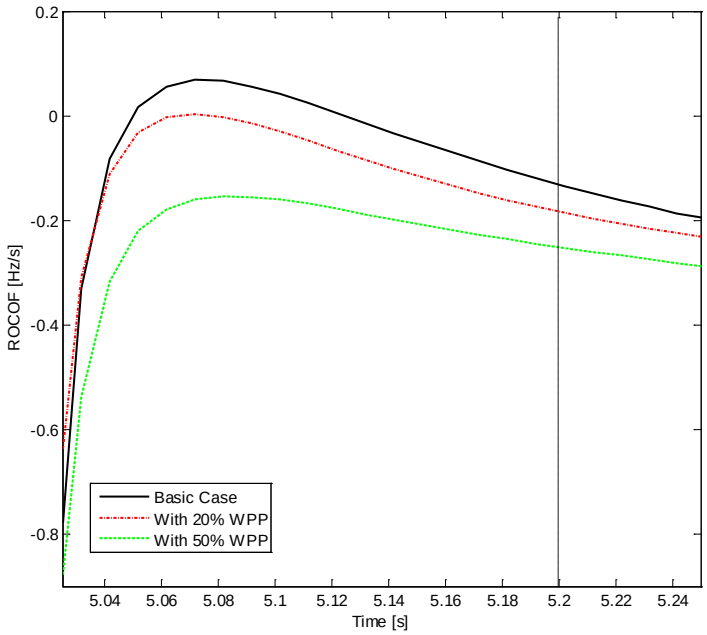

Figure 14: ROCOF during 200ms after the largest infeed loss

Figure 15 illustrates the system frequency measured at the generator G1, the electrical power generated by each WPP, their available power and inertial response contribution. Notice that the electrical powers generated by all WPPs during the IR event are similar. Due to the power reserve existing in the WPPs, during IR event, i.e. 0.1pu, overloading of WPP of 4% lasts less than 2.5s. The maximum of the inertial response contribution ΔP_{IR} of WPPs is 15% of the rated power. The wind turbine

enters for a very short period in overloading. However, as wind turbine is running at high wind speed, this does not yield to recovery period.

The WPP inertial response, power oscillation damping and synchronous power contribution, i.e. ΔP_{IR}, ΔP_{POD} and ΔP_{SP} respectively, while only IR ancillary service is activated for the 1.2pu wind speed is similar to that illustrated in Figure **10** for 0.86pu wind speed. This is due to the fact that the number of wind turbines in WPPs for 0.86pu case is increased in order to match the same load flow as that for 1.2pu case in 20% and 50% wind power penetration scenarios.

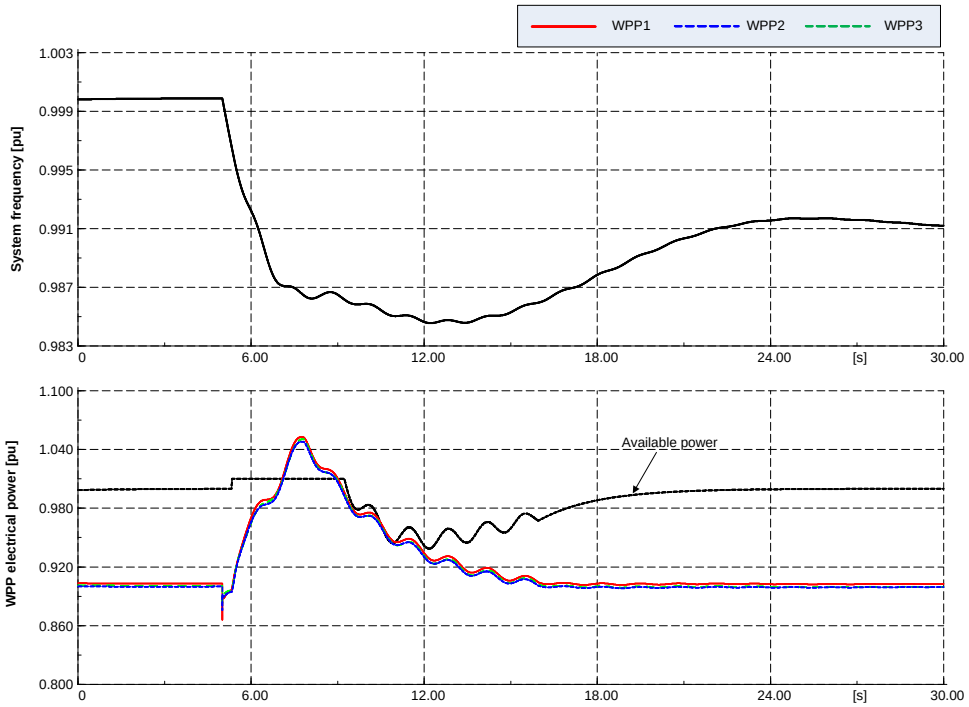

Figure 15: Frequency excursion, WPPs electrical power and ΔP_{IR} **of** WPPs during IR event – for 1.2pu wind speed and 50% wind power penetration scenario.

Figure 16 illustrates the wind turbine performance during the grid frequency deviation, while the IR control functionality is activated for 50% wind power penetration scenarios at a high wind speed of 1.2pu.

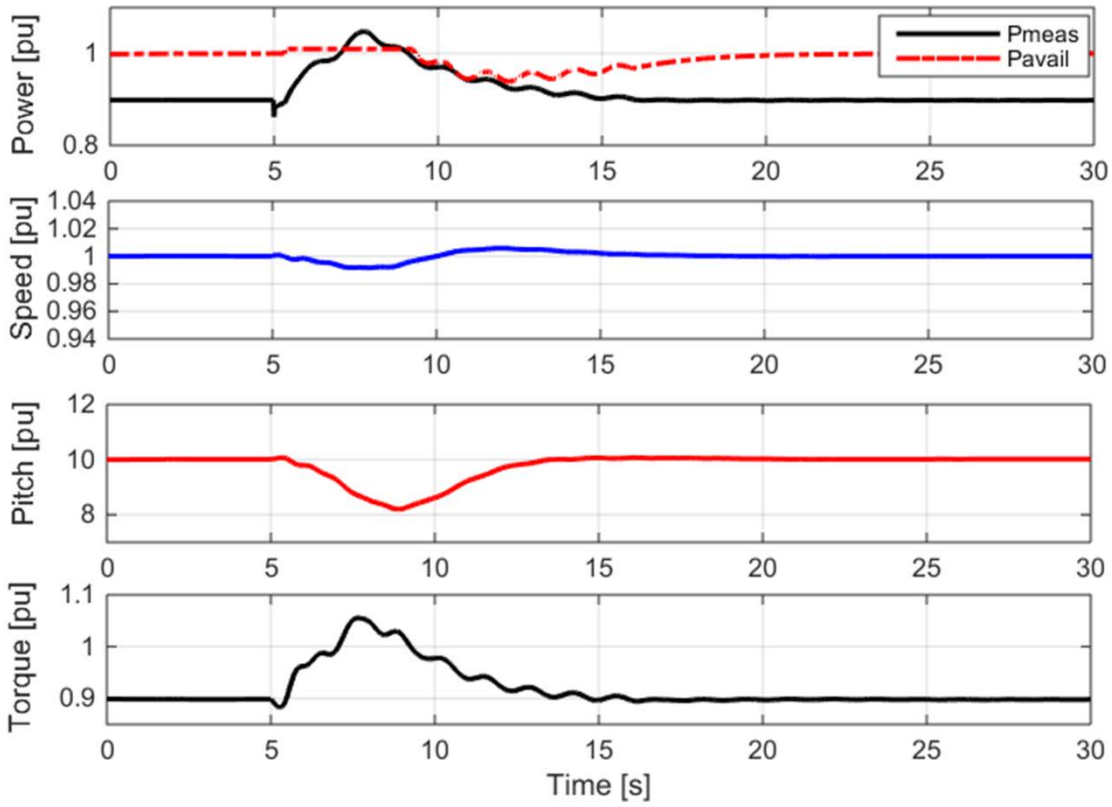

Figure 16: Wind turbine performance at **1.2pu wind speed** during IR event – 50% wind power penetration scenarios.

The illustrated signals are the electrical power and available power, generator speed, pitch angle and shaft torque. As mentioned before, the wind turbine is running with a 10% curtailment. During the frequency excursion, the wind turbine contributes with additional power in order to support the grid. The temporary surplus of electrical power generated by the turbine makes it to decelerate in order to compensate for the temporary imbalance between the electrical and mechanical power. However, this deceleration is not as significant as in the case of running the wind turbine at low wind speed during the frequency excursion as shown in Figure 11. The reason, as also depicted in Figure **16** , is that at high wind speed the turbine has the possibility to increase its aerodynamic power, by decreasing its pitch in order to reduce the power imbalance during overproduction. The effect of decreasing the pitch angle is also visible in the shaft torque, which, as result, is increased with about 15% compared with its initial value.

Notice also that the power reserve of the WT is slightly exceeded. As shown in Figure **16** , the pitch angle is not reduced at its minimum value (i.e. 0deg) even for the 50% wind power penetration case when the turbine's reserve is quickly consumed. This implies that the pitch angle can still be used to compensate for the power imbalance in case an even higher power surplus is required.

The rotational speed reaches its rated value before the overproduction is completed and even presents a slight overshoot. The recovery period of the WT after overproduction is as expected almost negligible at high wind speeds, as the electrical power returns directly to its rated value when the overproduction is completed.

Beside the performance of the wind turbine while providing system support like IR response, it is also of high importance to understand how the WPP contributions in terms of inertial response, power oscillation damping and synchronous power, i.e. ΔP_{IR}, ΔP_{POD} and ΔP_{SP} respectively, look in respect to each other. Are they working in opposite directions, then their sum may produce a zero power contribution. Are they additive, then their sum may exceed the power available in case when they are all enabled. Once experience with only one enabled control functionality is established, this knowledge may be relevant in case of studying simultaneous or sequential activation of multiple ancillary services.

In addition to the conclusions stated above, the simulation results are summarized in Table **5** for partial and full load, respectively. The operational metrics are represented by minimum frequency point (nadir), ROCOF at 200ms after the largest infeed loss, i.e. G2 and the frequency oscillation amplitude (in 50 Hz base). As it can be seen in Table 5, the ROCOF is not changing within a given penetration scenario due to the df/dt controller gain and the detection time.

Wind power penetration	Inertial response (IR) contribution from WPPs			Frequency nadir [pu]	ROCOF [Hz/s]	Amplitude [pu]
	WPP1	WPP2	WPP3			
0%	not connected			0.984	0.132	0.001
20%	no IR	not connected	not connected	0.983	0.184	0.001
	with IR			0.987	0.184	0.0007
50%	no IR	no IR	no IR	0.977	0.251	0.001
	with IR	no IR	no IR	0.982	0.251	0.001
	with IR	with IR	no IR	0.983	0.251	0.001
	with IR	with IR	with IR	0.985	0.251	0.0008

Table 5: Operational metrics.

In the above figures and the related explanations, the number of turbines in WPPs is increased for the 10 m/s case to match the same load flow as the 14 m/s case in 20% and 50% wind penetration scenarios. Furthermore, to investigate the impact of the wind speed the case where the same number of turbines is kept same as in the 14 m/s case is simulated for the 20% wind penetration scenario. The simulation results are shown in **Figure 17**.

The frequency deviation is same with 14m/s case due to the available reserve. As it can be seen from the simulation results, the active power reserve is sufficient enough for the 10m/s case to provide the required frequency support according to the inertial response control parameters and the frequency deviation. The available power estimation block supplies an extra amount of reserve power that is used for the inertial response of the WPP. In this and also in the previous simulations, during the inertial response the wind turbine is switched to the overloading mode (See Figure) which is going to provide the required amount of active power from the WPP controller.

Therefore, it may cause the wind turbine to go to the recovery period, unless there is a sufficient amount of active power reserve.

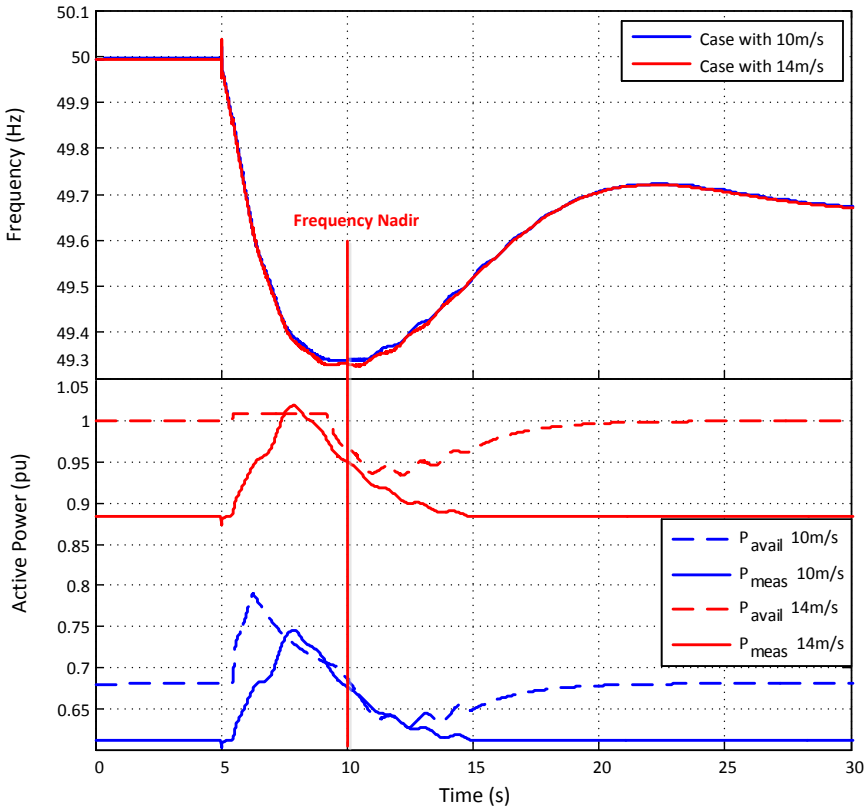

Figure 17: Frequency and active power comparison between partial and full load operation case for the same number of wind turbines

5 Power oscillation Damping (POD)

POD is typically an embedded feature in the power system stabiliser of synchronous generators. It damps the oscillations in the power system. The displacement of conventional power plants in the future by WPPS may require this service product to be delivered by WPPs.

5.1 POD controller

The goal of this control functionality inside WPP is to demonstrate that a WPP can be used as a damping device for the power oscillating in a power system- similar to the PSS in the conventional power plants. A WPP may be used as a damping device by modulating either active or reactive power output.

The input to the POD controller can typically be a signal which reflects the power system oscillations. Two input signals, i.e. current magnitude and active power flow, have been used in the present investigation. The WPP can provide POD by modulating either active and/or reactive power, i.e. ΔP_{POD} and ΔQ_{POD}. These additional active and

reactive power contributions are summed up with the overall power references provided by the WPPC [1].

POD controller consists typically of a Wash-Out filter, a Lead-Lag, a Gain and a limiter for the output signal. The Washout filter is filtering the input signal and removes any high order harmonics that are not of interest. The Lead-Lag block is providing the proper phase compensation desired. It consists of two stage phase compensation and a gain that compensate the attenuation at the desired frequency for which the lead-lag is tuned. The gain is scaling the output to obtain the desired contribution for POD control. The reference signal from POD is limited to the available range allocated for POD.

5.2 Definition of simulation test cases for POD

For each wind penetration scenario, other than 0%, the POD control is tested for different input/output signals. A complete list of the simulation test cases proposed for POD, locally or remotely, and of the signals measured is given in Table **6**. The simulation test cases are illustrated only for 1.2pu wind speed, as similar results are obtained for 0.86pu wind speed.

PoM	% wind power	POD input signal	POD ouput signal	POD parameters	POD describtion	TC_PODi
Remote measurement Line 6-1	20%	Current magnitude	ΔQ_{POD}	POD_P1	I & ΔQ_{POD}	TC_POD1
		Active power	ΔP_{POD}	POD_P2	P & ΔP_{POD}	TC_POD2
	50%	Current magnitude	ΔQ_{POD}	POD_P1	I & ΔQ_{POD}	TC_POD3
		Active power	ΔP_{POD}	POD_P2	P & ΔP_{POD}	TC_POD4
Local measurement closed to PCC : WPP1: Line 5-2 (Bus 5)	20%	Current magnitude	ΔQ_{POD}	POD_P3	I & ΔQ_{POD}	TC_POD5
		Active power	ΔP_{POD}	POD_P4	P & ΔP_{POD}	TC_POD6
		Active power	ΔQ_{POD}	POD_P4	P & ΔQ_{POD}	TC_POD7
Local measurement closed to PCC: WPP1: Line 5-2 (Bus 5) WPP2: Line 7-8 (Bus 8) WPP3: Line 4-6 (Bus 4)	50%	Current magnitude	ΔQ_{POD}	POD_P3	I & ΔQ_{POD}	TC_POD8
		Active power	ΔP_{POD}	POD_P4	P & ΔP_{POD}	TC_POD9
		Active power	ΔQ_{POD}	POD_P4	P & ΔQ_{POD}	TC_POD10

Table 6: Simulation test cases for POD.

5.3 Parameters of the POD controller

The parameters of the POD controller, tuned mainly for 20% wind power penetration scenario in the work done in WP1, are used. Furthermore, the communication delays are not included in the implementation of the controllers, as they are assumed compensated.

5.4 Success criteria

The POD functionality in WPPs aims to find answer to the question how much power (P/Q) modulation from WPPs is necessary in order to provide an effective damping of power oscillations? Besides the overall design criteria, the effectiveness of POD functionality shall be evaluated based on the following success criteria:

Characterization	Specifications	Success Criterion
Damping	POD control shall achieve at least 5% damping ratio on all harmonic components of the monitored variable	POD-SC-01
Mode Shapes	No significant changes in the frequencies of natural modes (i.e. without damping control)	POD-SC-02
Stability	Voltage at PCC remains in normal operation band during the damping control action.	POD-SC-03

Table 7: Success criteria for POD [4].

As depicted in Table 6, the test cases for POD are carried out for two wind power penetration scenarios (i.e. 20% and 50%), different inputs/outputs (i.e. current magnitude and active power flow) and two types of measurements (PoM), namely remote and local.

5.5 POD test cases – simulations with remote measurement

5.5.1 20% wind penetration - POD Simulations with remote PoM on Line 6-1

In the 20% wind penetration scenario only one WPP, i.e. WPP1, is connected to the power system in Figure 4, namely at Bus 5.

Figure 19, Figure 20 and Figure 21 reflect the performance of POD for 20% wind penetration case with remote measurement, namely for the test cases TC_POD_1 and TC_POD_2.

Figure 19 illustrates the impact of the POD controller on its input signals namely current magnitude or active power for the two test cases corresponding 20% wind power penetration. In both cases the POD controller damps the oscillations of remote measurements of current and active power in Line 6-1, respectively.

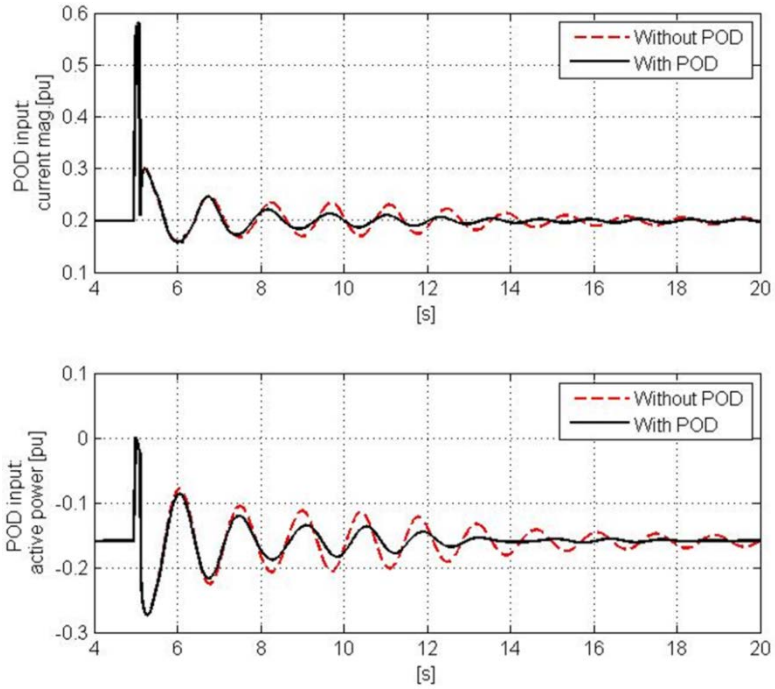

Figure 18: Input signals (current and active power) of the POD controller with and without POD for TC_POD$_1$ and TC_POD$_2$

Figure 20 illustrates the input and output waveforms for the POD controller, when current magnitude and active power flow are used as input respectively, for the test cases TC_POD$_1$ and TC_POD$_2$. Notice that in TC_POD$_1$, the output of the POD controller damps the input signal without reaching its maximum limits of +/- 0.1pu, as it is the case of TC_POD$_2$, where active power is used as input signal in the POD controller. The input and outputs in these two cases are also in opposite phase.

Figure 21 illustrates the active and reactive power of the WPP1, namely the only WPP connected in the 20% wind power penetration scenario. The figure reflects the power measurement, power reference and available power. Notice that in both test cases TC_POD$_1$ and TC_POD$_2$, the WPP has enough power reserve to be able to contribute with POD. The available power in TC_ POD$_2$, implemented as described in [1], depends both on the wind speed and on the active power reference changings. Notice that the plant is also capable of following well its reference with a certain ramp-up value at the 0.7 Hz. The results indicate no stationary offsets and a phase-lag of approximately 0.1 sec (communication delays are not included).

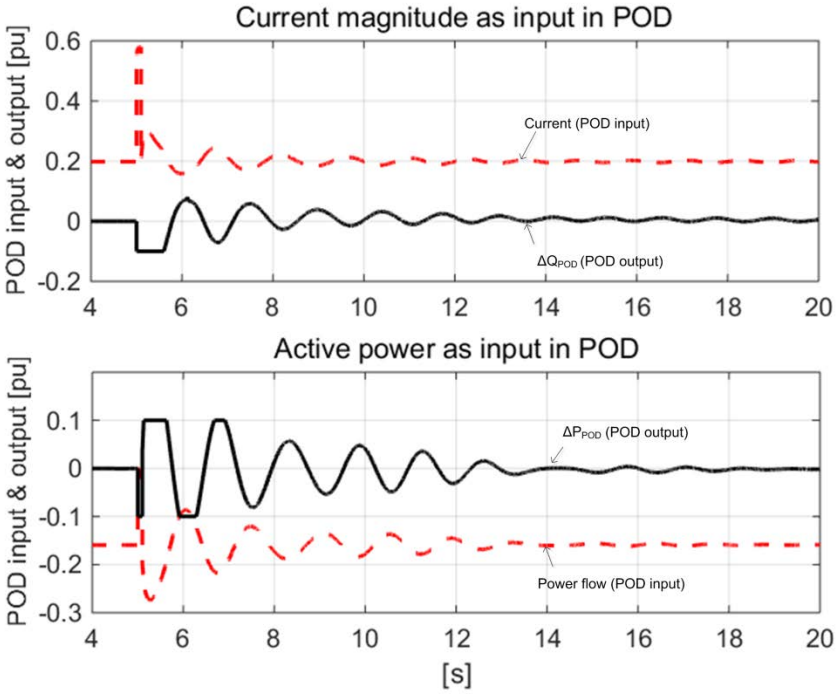

Figure 19: Waveforms of input and output of the POD controller for TC_POD_1 and TC_POD_2.

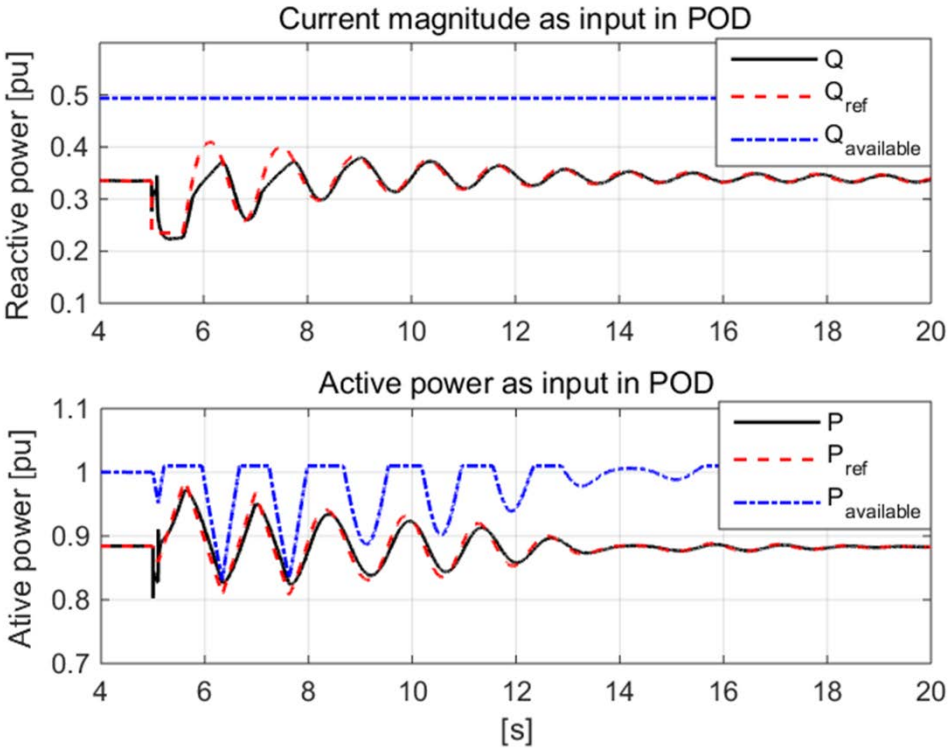

Figure 20: Active and reactive power of aggregated wind turbine in TC_POD_1 and TC_POD_2.: measurement, reference and available.

The impact of using different types of POD controller, namely POD – I&ΔQ and POD - P&ΔP with current or active power as input signal respectively, on the remote

measurements in Line 1-6, i.e. current and active power, is depicted both in Figure 22 and in Table 9.

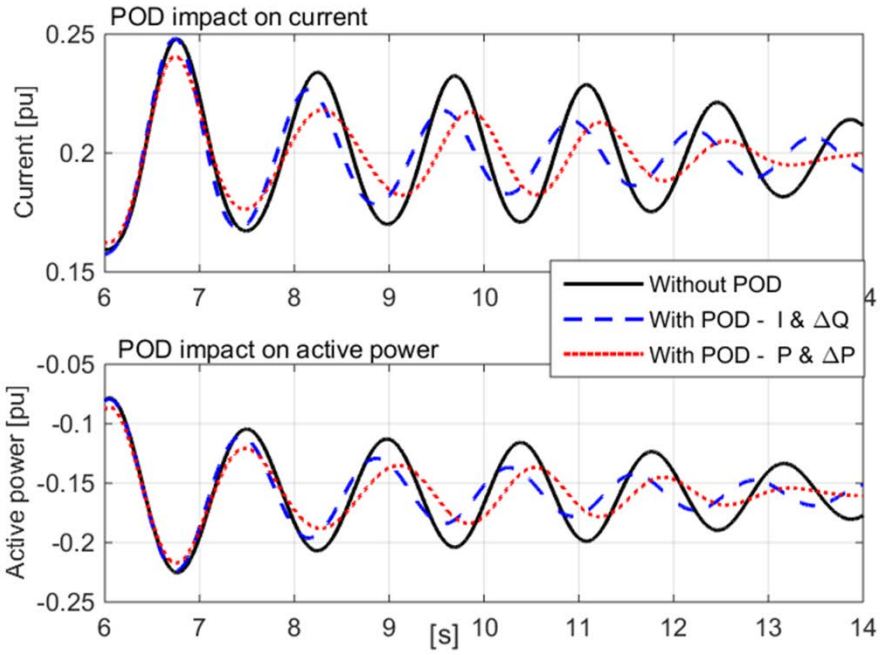

Figure 21: Impact on current and power measured remotely in Line 1-6 of using POD-I&ΔQ_{POD} or POD- P&ΔQ_{POD} for 20%wind power penetration.

It is worth noticing that for 20% wind power penetration case when only WPP1 is connected to the power system, the POD controller has a positive damping effect on the current and active power flow in Line 6-1, no matter its input signal. As depicted in Table 9, POD controller with active power as input signal (i.e. POD - P& ΔP) has bigger damping impact on the power measured in the remote Line 1-6, without implying significant changes in the frequencies of natural modes. Its damping ratio is more than doubled up compared with the case without POD.

20%	**Without POD**		**POD - I & ΔQ**		**POD - P & ΔP**	
Signals	Frequency [Hz]	Damping (%)	Frequency [Hz]	Damping (%)	Frequency [Hz]	Damping (%)
Power	0.7	**4.3**	0.72	**7.7**	0.7	**9.6**
Current	0.71	**2.8**	0.7	**8.1**	0.7	**8.2**

Table 8: The damping frequency and ratio of the active power and current in Line 6-1 – 20% scenario with and without POD controller.

Notice also that the two POD controllers have an equal impact on the current in Line 1-6. The current is almost damped three times more compared with the case without POD.

5.5.2 50% wind penetration - POD Simulations with remote PoM on Line 6-1

In the 50% wind penetration scenario three WPPs, i.e. WPP1 at Bus 5, WPP2 at Bus 8 and WPP3 at Bus 4, are connected to the power system illustrated in Figure 4. The simulation test cases for POD for 50% wind penetration scenario are performed using the controller parameters depicted in Table 7, tuned basically for the 20% wind power

penetration case. The test cases are investigated both for the situations when POD contribution is only from one WPP and when all WPPs are contributing simultaneously with POD.

5.5.2.1 POD only activated in WPP1

Figure 23 illustrates the impact of the POD controller on its input signals namely current magnitude or active power in Line 6-1 respectively, for the test cases TC_POD$_3$ (I&ΔQ_{POD}) and TC_POD$_4$ (P&ΔP_{POD}) when only POD in WPP1 is activated.

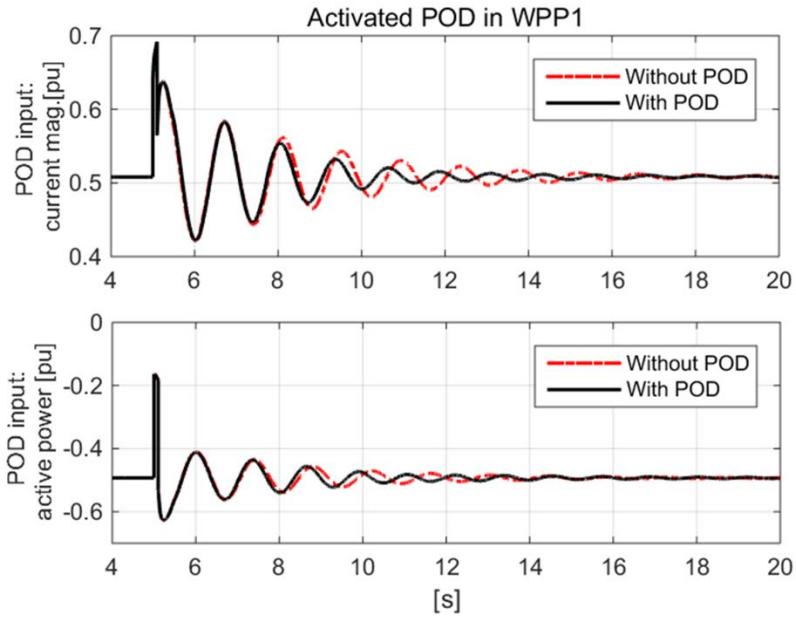

Figure 22: Input signals (current and active power) of the POD controller only activated in WPP1 with and without POD for TC_POD$_3$ and TC_POD$_4$

As depicted in Table 10, POD controller with current as input signal (i.e. POD - I& ΔQ_{POD}) has slightly bigger damping impact on the current and active power measured in the remote Line 1-6, without implying significant changes in the frequencies of natural modes.

50% - WPP1	Without POD		POD - I & ΔQ		POD - P & ΔP	
Signals	Frequency [Hz]	Damping (%)	Frequency [Hz]	Damping (%)	Frequency [Hz]	Damping (%)
Power	0.71	**6.5**	0.74	**7.4**	0.76	**6**
Current	0.71	**6.1**	0.74	**6.7**	0.76	**5.4**

Table 9: The damping frequency and ratio of the active power and current in Line 6-1 – 50% scenario with and without POD controller- only in WPP1.

Similar results as those described in Section 5.5.1 regarding the POD controllers' input/output waveforms and the active/reactive power of WPP, during POD contribution in TC_POD$_3$ and TC_POD$_4$ are illustrated in Appendix A (i.e. Figure 49 and Figure 50).

5.5.2.2 POD only activated in WPP2

Figure 24 illustrates the impact of the POD controller on its input signals namely current magnitude or active power in Line 6-1, for the test cases TC_POD$_3$ (I&ΔQ_{POD}) and TC_POD$_4$ (P&ΔP_{POD}) when only POD in WPP2 is activated.

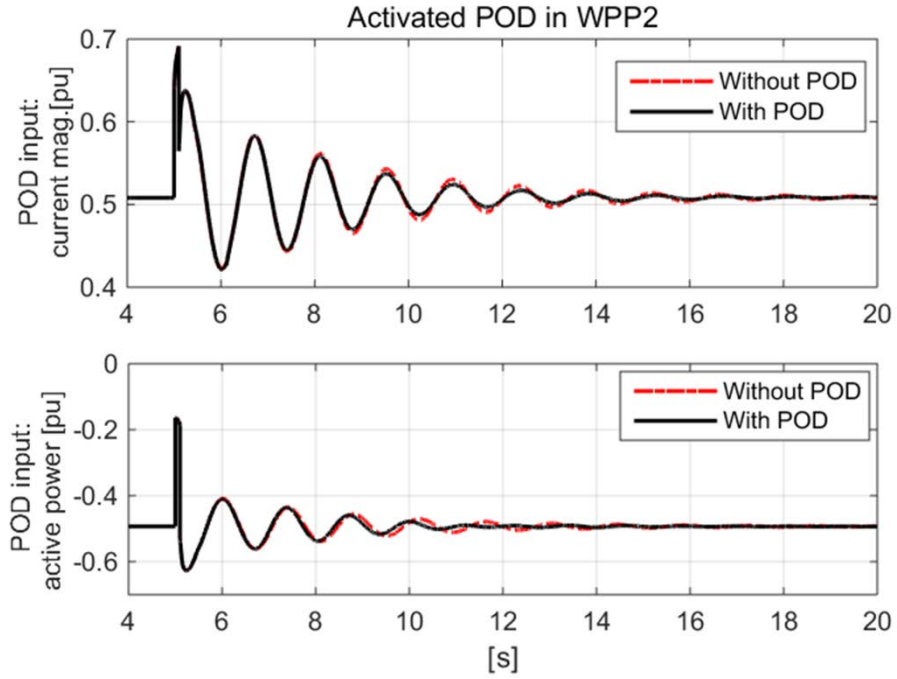

Figure 23: Input signals (current and active power) of the POD controller only activated in WPP2 with and without POD for TC_POD$_3$ and TC_POD$_4$

As depicted in Table 11, POD controller with active power as input signal (i.e. POD - P& ΔP_{POD}) has almost no damping effect on the current and active power measured in the remote Line 1-6. The POD – I& ΔP_{POD} has also a very small impact on the damping of the remote measured signals in Line 6-1. No significant changes in the frequencies of natural modes occur while using POD controllers.

50% - WPP2	Without POD		POD - I & ΔQ		POD - P & ΔP	
Signals	Frequency [Hz]	Damping (%)	Frequency [Hz]	Damping (%)	Frequency [Hz]	Damping (%)
Power	0.71	**6.5**	0.72	**7.1**	0.74	**6.9**
Current	0.71	**6.1**	0.72	**6.6**	0.74	**6.2**

Table 10: The damping frequency and ratio of the active power and current in Line 6-1 – 50% scenario with and without POD controller- only in WPP2.

Similar results as those described in Section 5.5.1 regarding the POD controllers' input/output waveforms and the active/reactive power of WPP, during POD contribution in TC_POD$_3$ and TC_POD$_4$ are illustrated in Appendix A (i.e. **Figure** 51 and Figure 52**).**

5.5.2.3 POD only activated in WPP3

Figure 25 illustrates the impact of the POD controller on its input signals namely current magnitude or active power in Line 6-1, for the test cases TC_POD$_3$ (I&ΔQ_{POD}) and TC_POD$_4$ (P&ΔP_{POD}) when only POD in WPP3 is activated.

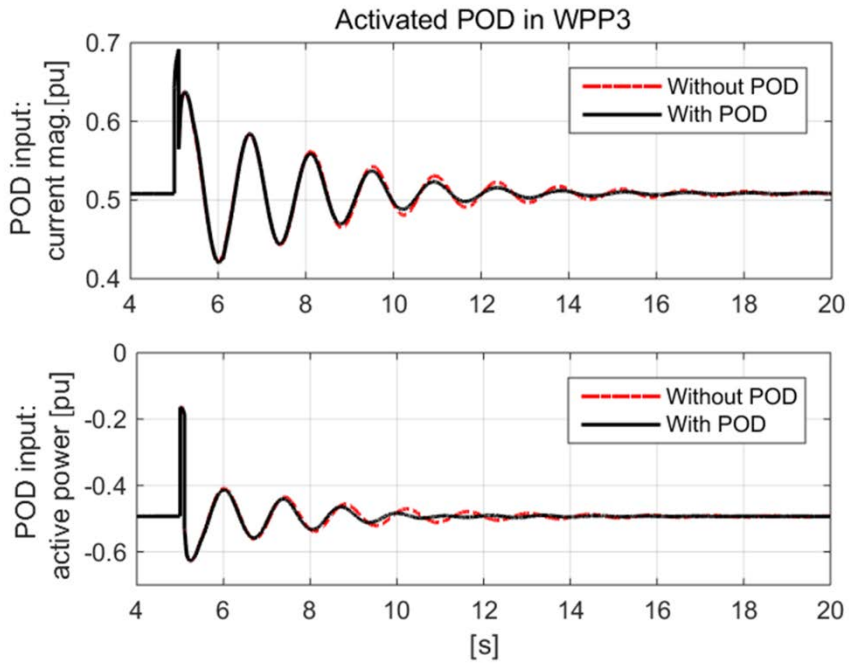

Figure 24: Input signals (current and active power) of the POD controller only activated in WPP3 with and without POD for TC_POD$_3$ and TC_POD$_4$.

As depicted in Table 12, POD controller with active power as input signal (i.e. POD - P& ΔP_{POD}) has slightly better damping effect both on the current and active power measured in the remote Line 1-6, than the POD – I& ΔP_{POD} controller. No significant changes in the frequencies of natural modes occur while using POD controllers.

50% - WPP3	Without POD		POD - I & ΔQ		POD - P & ΔP	
Signals	Frequency [Hz]	Damping (%)	Frequency [Hz]	Damping (%)	Frequency [Hz]	Damping (%)
Power	0.71	**6.5**	0.72	**7.1**	0.74	**7.5**
Current	0.71	**6.1**	0.72	**6.6**	0.74	**6.9**

Table 11: The damping frequency and ratio of the active power and current in Line 6-1 – 50% scenario with and without POD controller- only in WPP3.

Similar results as those described in Section 5.5.1 regarding the POD controllers' input/output waveforms and the active/reactive power of WPP, during POD contribution in TC_POD$_3$ and TC_POD$_4$ are illustrated in Appendix A (i.e. Figure 53 and Figure 54).

5.5.2.4 POD activated simultaneously in WPP1, WPP2 and WPP3

Figure 26 illustrates the impact of the POD controller on its input signals namely current magnitude or active power in Line 6-1 respectively, for the test cases TC_POD$_3$ (I&ΔQ_{POD}) and TC_POD$_4$ (P&ΔP_{POD}) when all three wind power plants WPP1, WPP2 and WPP3 are contributing with POD. The simulation test cases are carried out by assuming that the same type of POD controller (i.e. same input/output signals + same parameters) is used in all WPPs.

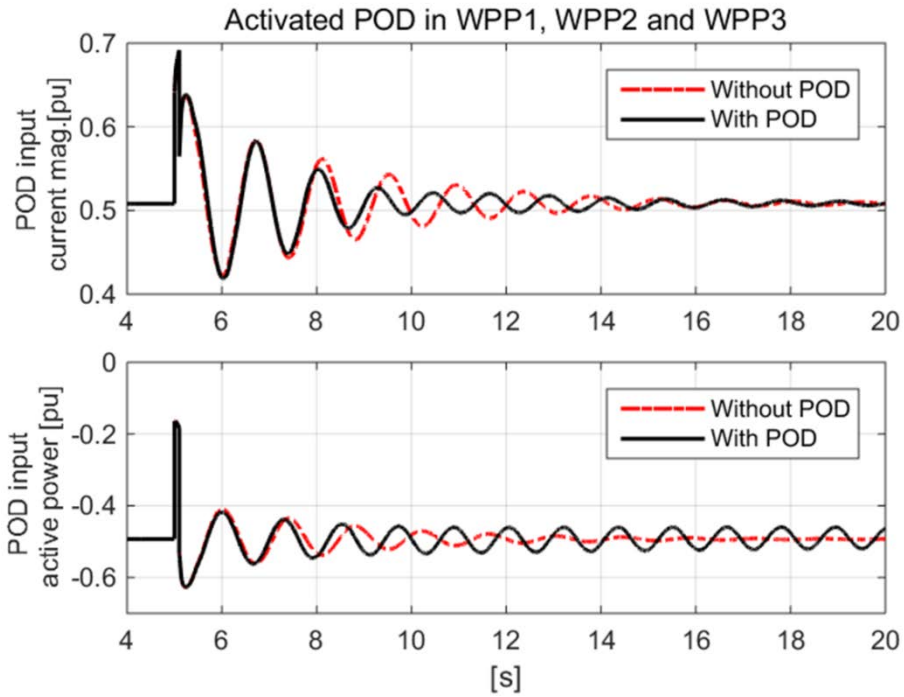

Figure 25: Input signals (current and active power) of the POD controller activated in WPP1, WPP2 and WPP3, with and without POD for TC_POD$_3$ and TC_POD$_4$.

Both Figure 26 and Table 13 indicate that when the POD controllers are enabled in all three WPPs simultaneously, the damping impact on the power and current signals is very bad when the active power is used as input in the POD controller (i.e. POD - P& ΔP_{POD}). Actually the damping of current and power, when POD - P& ΔP_{POD} is used, is almost two times lower than the case without POD. The POD – I& ΔQ_{POD} controller damps slightly better compared without POD case. No significant changes in the frequencies of natural modes occur while using POD controllers.

50% - WPP1,2,3	**Without POD**		**POD - I & ΔQ**		**POD - P & ΔP**	
Signals	Frequency [Hz]	Damping (%)	Frequency [Hz]	Damping (%)	Frequency [Hz]	Damping (%)
Power	0.71	**6.5**	0.75	**8.2**	0.82	**2.8**
Current	0.71	**6.1**	0.76	**7.3**	0.82	**2.5**

Table 12: The damping frequency and ratio of the active power and current in Line 6-1 – 50% scenario with and without POD controller - in WPP1,2,3.

The results that the damping can be worsen when all WPPs contribute with POD indicate that the coordination between these controllers is of high relevance.

The results for TC_POD$_3$ and TC_POD$_4$ on the POD controllers' input/output waveforms and on the active and reactive power of WPP1, WPP2 and WPP3 respectively, during POD contribution are illustrated in Appendix A (i.e. Figure 55 and Figure 56).

In addition to the conclusions stated above, the simulation results are summarized in Table 14 for the impact of POD on current and active power signals, respectively.

	Without POD		With POD	POD - I & ΔQ		POD - P & ΔP	
Current	Frequency [Hz]	Damping (%)		Frequency [Hz]	Damping (%)	Frequency [Hz]	Damping (%)
	0.71	**6.1**	**WPP1 only**	0.74	**6.7**	0.76	**5.4**
			WPP2 only	0.72	**6.6**	0.74	**6.2**
			WPP3 only	0.72	**6.6**	0.74	**6.9**
			WPP1, WPP2, WPP3	0.76	**7.3**	0.82	**2.5**
	Without POD		**With POD**	**POD - I & ΔQ**		**POD - P & ΔP**	
Power	Frequency [Hz]	Damping (%)		Frequency [Hz]	Damping (%)	Frequency [Hz]	Damping (%)
	0.71	**6.5**	**WPP1 only**	0.74	**7.4**	0.76	**6**
			WPP2 only	0.72	**7.1**	0.74	**6.9**
			WPP3 only	0.72	**7.1**	0.74	**7.5**
			WPP1, WPP2, WPP3	0.75	**8.2**	0.82	**2.8**

Table 13: 50% wind power penetration case - Active power and current damping frequency and ratio in Line 6-1 with and without POD controller.

Based on the assumptions defined for the present test cases, the following general remarks can be done when remote measurements are used as inputs in the POD controller:

- The POD – I & ΔQ_{POD} controller has in general better damping impact on the current and active power, measured remotely in Line 6-1, than the POD – P & ΔP_{POD} controller.
- When POD – I & ΔQ_{POD} controller is used in only one WPP per time, the damping ratio on current and active power in Line 6-1 is slitly better than the case without any damping.
- Using POD – I & ΔQ_{POD} controller enabled in all WPPs simultaneously, has slightly better damping effect than the case when it is enabled in only one WPP per time.
- The POD – P & ΔP_{POD} controller has a better damping effect only when it is enabled in WPP2 and WPP3. A better parameter tuning might improve the performance.
- When all three different WPPs, having the same parameters in their POD controllers are required to contribute with POD functionality, the POD – P & ΔP_{POD} controller is not the best solution. A coordinated tuning of the POD controller for each WPP might be necessary when the active power signal is used as input in the POD controller. This fact might be difficult to implement in practice, as the WPPs might have different owners. The POD ancillary service cannot be directly imposed as a requirement in grid codes without system wide studies.

5.6 POD test cases – simulations with local measurements

5.6.1 20% wind penetration - POD Simulations with local measurement

Figure **27** illustrates the impact of the POD controller on its input signals namely current magnitude or active power for the test cases TC_POD_5 (I&ΔQ_{POD}), TC_POD_6 (P&ΔP_{POD}) and TC_POD_7 (P&ΔQ_{POD}) defined in Table **6** for 20% wind penetration case with local measurement. In all three cases the POD controller damps the oscillations of local measurements of current and active power in Line 6-1, respectively.

The POD controllers' input/output waveforms and the active and reactive power of WPP1 during POD contribution in test cases TC_POD$_5$, TC_POD$_6$ and TC_POD$_7$ are illustrated in Appendix B (i.e. Figure 57 and Figure 58).

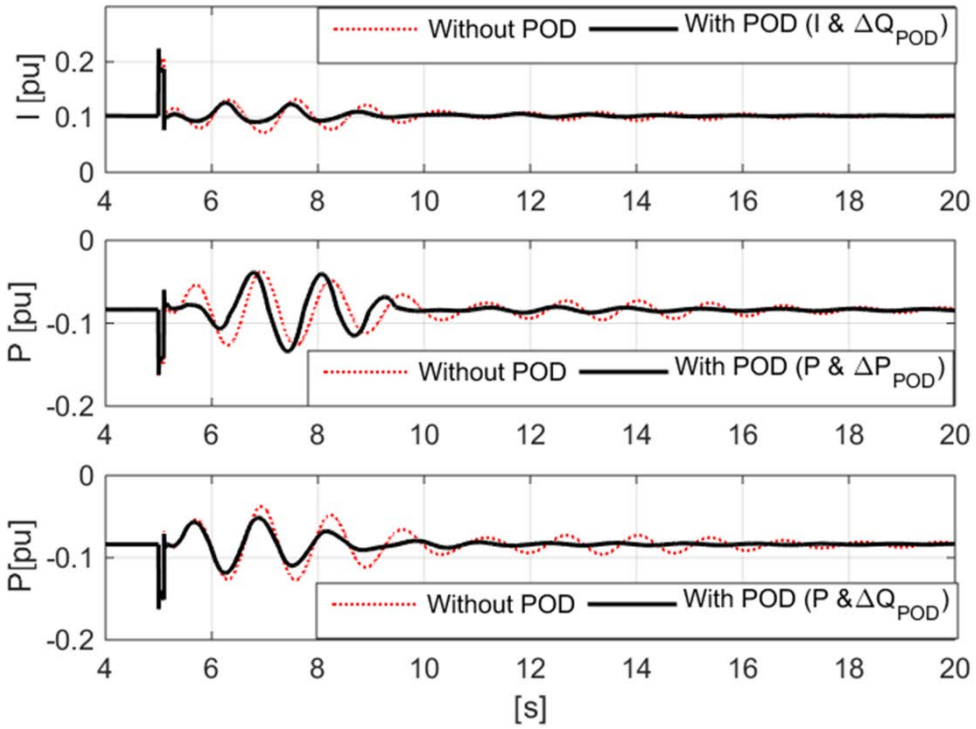

Figure 26: Input signals (current and active power) of the POD controller with and without POD for TC_POD$_5$, TC_POD$_6$ and TC_POD$_7$.

The impact on the current and active power in Line 5-2 of the POD controller, using the three types of input/output pairs for POD, i.e. POD - I&ΔQ_{POD}, POD - P&ΔP_{POD} and P&ΔQ_{POD}, is both illustrated in Figure 28 and in Table 15.

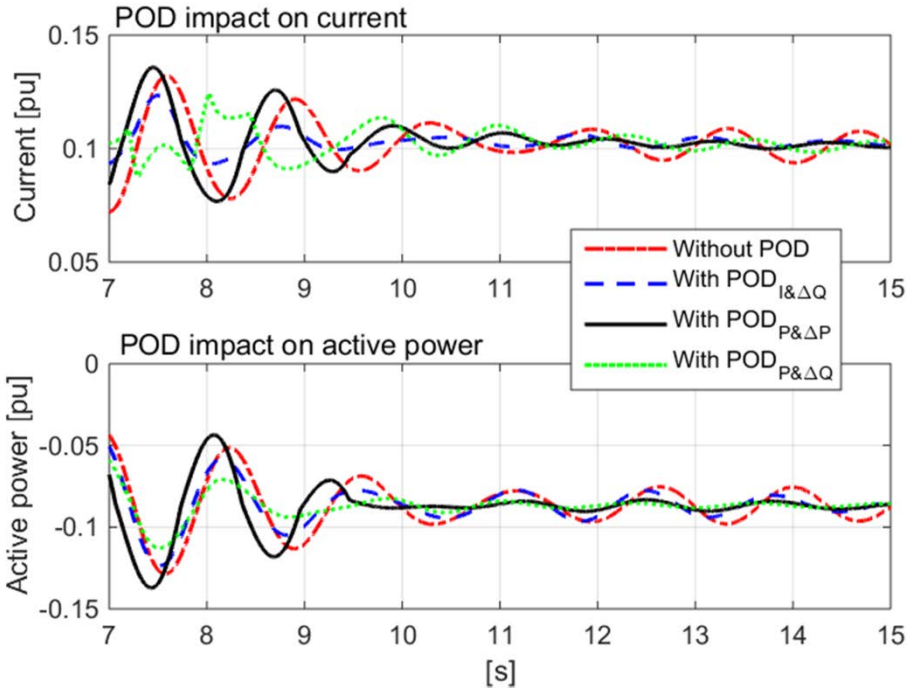

Figure 27: Impact of the three types of POD controllers (I&$\Delta Q_{POD,,}$ P&ΔQ_{POD} and P&ΔQ_{POD}) activated in WPP1 for 20% wind power penetration, on current and power measured locally in Line 5-2.

It is worth noticing that for 20% wind power penetration case, when only one WPP is connected to the power system, the POD controller has a positive damping effect on the current and active power flow in Line 5-2, no matter input signal. As depicted in Table 15, POD controller with active power as input signal (i.e. POD - P&ΔP_{POD}) has bigger damping impact on the power measured in the remote Line 5-2, without implying significant changes in the frequencies of natural modes.

As depicted in Table 9, POD controllers with active power as input signal (i.e. POD - P&ΔP_{POD} and POD - P&ΔQ_{POD}) have bigger damping impact on the power measured locally in Line 5-2, than the POD controller using current as input signal. Notice that all POD do not imply significant changes in the frequencies of natural modes.

20%	**Without POD**		**POD - I & ΔQ**		**POD - P & ΔP**		**POD - P & ΔQ**	
Signal	Frequency [Hz]	Damping (%)	Frequency [Hz]	Damping (%)	Frequency [Hz]	Damping (%)	Frequency [Hz]	Damping (%)
Power	0.7	**3.7**	0.71	**6**	0.76	**20.4**	0.7	**14.1**
Current	0.68	**4.2**	0.74	**9.1**	0.8	**16.2**	0.68	**10.8**

Table 14: The damping frequency and ratio of the active power and current in Line 5-2 – 20% scenario with and without POD controller.

The figures in the table are very well in concordance with the performance results illustrated in Figure 28. The POD - P& ΔP_{POD} controller has biggest damping impact on the current in Line 5-2, while the other two POD controllers have almost similar damping ratio. The voltage variation of Bus5 is ±4% at the pre-fault value for the POD P& ΔQ_{POD}, which is acceptable.

5.6.2 50% wind penetration - POD Simulations with local measurement

In the 50% wind penetration scenario three WPPs, i.e. WPP1 at Bus 5, WPP2 at Bus 8 and WPP3 at Bus 4, are connected to the power system illustrated in Figure 4. The simulation test cases for POD for 50% wind penetration scenario are performed using the controller parameters depicted in Table 7, tuned basically for the 20% wind power penetration case. The test cases are investigated both for the situations when POD contribution is only from one WPP and when all WPPs are contributing simultaneously with POD.

5.6.2.1 POD only activated in WPP1

Figure **29** illustrates the impact of the POD controller on its input signals namely current magnitude or active power for the test cases TC_POD$_8$ (I&ΔQ_{POD}), TC_POD$_9$ (P&ΔP_{POD}) and TC_POD$_{10}$ (P&ΔQ_{POD}) defined in Table **6** for 50% wind penetration case with local measurement, when only POD in WPP1 is activated.

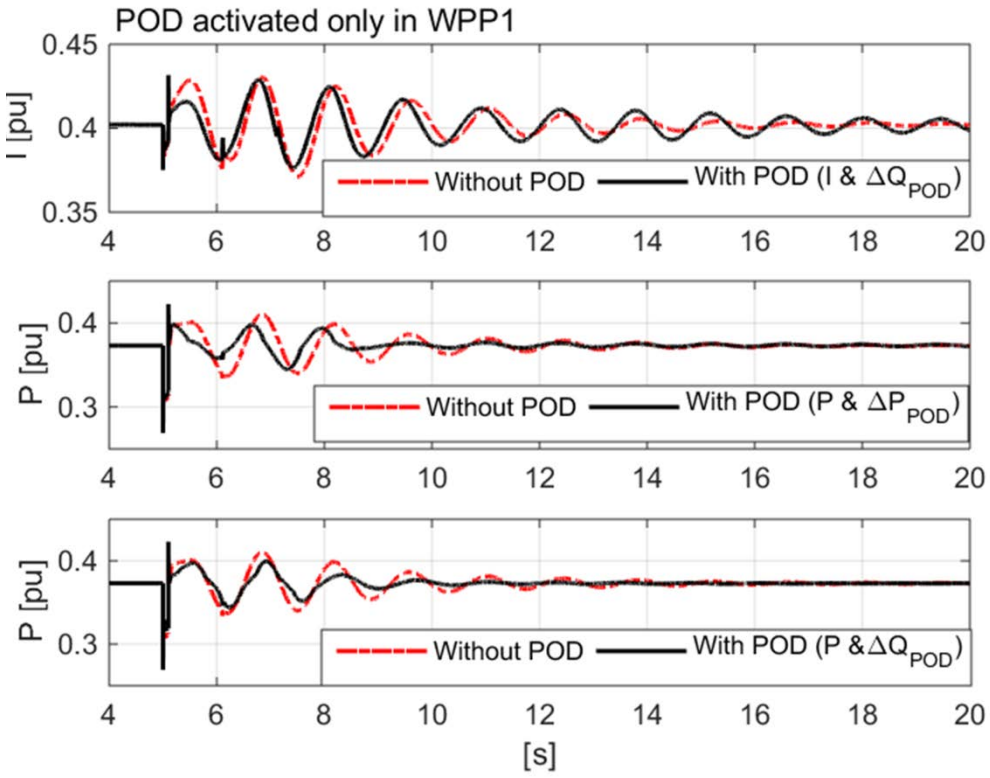

Figure 28: Input signals (current and active power in Line 5-2) of the POD controller with and without POD for TC_POD$_8$, TC_POD$_9$ and TC_POD$_{10}$ - POD activated only in WPP1.

Based on Figure 29, the following remarks can be done on the impact of the three types of POD controller, only activated in WPP1:

- POD - I&ΔQ_{POD} does not damp the oscillations of the current in Line 5-2
- POD - P&ΔP_{POD} does slightly damp the oscillations of active power in Line 5-2
- POD - P&ΔQ_{POD} does slightly damp the oscillations of the active power in Line 5-2

The POD controllers' input/output waveforms and the active and reactive power of WPP3, for the test cases TC_POD$_8$ (I&ΔQ_{POD}), TC_POD$_9$ (P& ΔP_{POD}) and TC_POD$_{10}$ (P&ΔQ_{POD}) defined in Table 6 for 50% wind penetration case with local measurement, when only POD in WPP1 is activated, are illustrated in Appendix B (i.e. Figure 59 and Figure 60).

The impact on the current and active power in Line 5-2 of the POD controller, using the three input/output configurations for POD controller, i.e. POD - I&ΔQ_{POD}, POD - P& ΔP_{POD} and P&ΔQ_{POD}, is illustrated in Figure 30 and in Table 16.

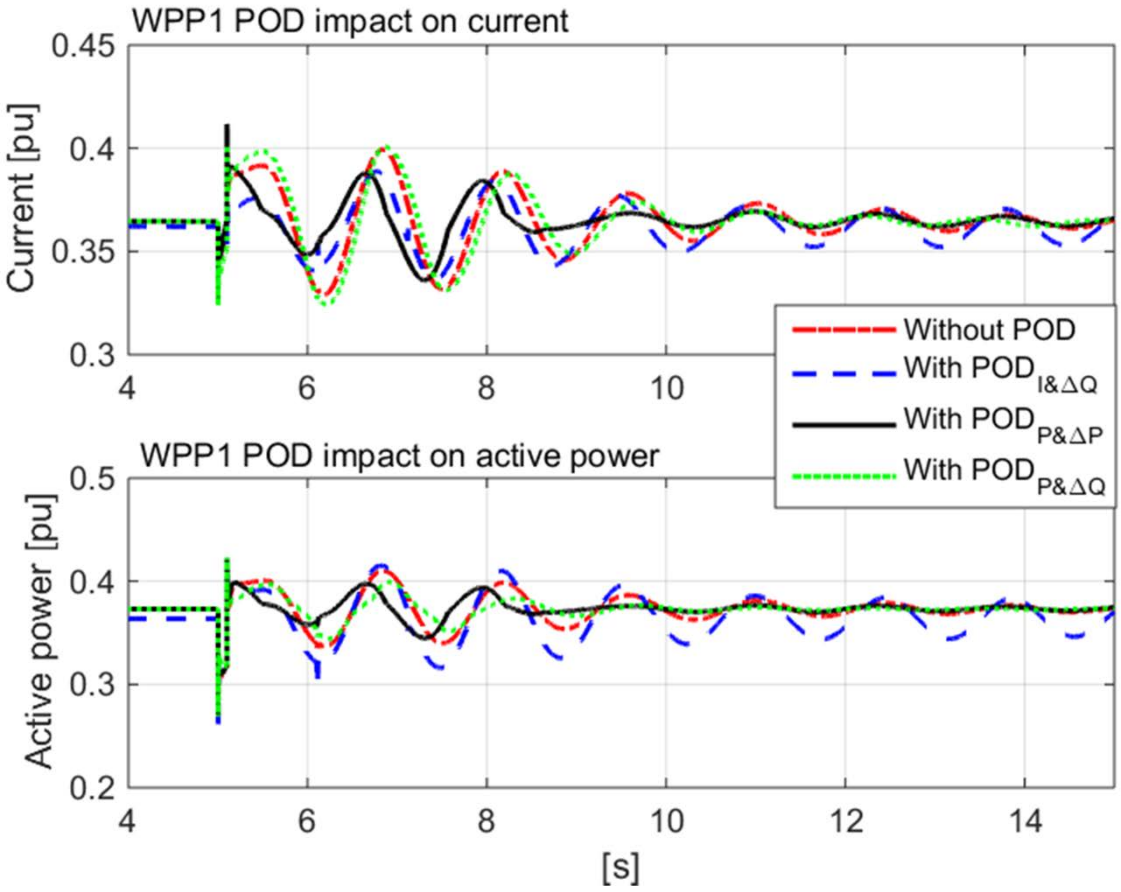

Figure 29: Impact on the current and power measured locally in Line 5-2 of using three different input/output pairs for POD controller (I&$\Delta Q_{POD,,}$ P&ΔQ_{POD} and P&ΔQ_{POD}) - 50% wind power penetration and POD only activated in WPP1.

The figures in the table are very well in concordance with the performance results illustrated in Figure 30. Notice that modulating reactive power with current as input signal into POD worsens the damping ratio both on current and on power. The best damping performance is given by modulating reactive power with active power as input into the POD controller.

50%-WPP1	Without POD		POD - I & ΔQ		POD - P & ΔP		POD - P & ΔQ	
Signal	Frequency [Hz]	Damping (%)	Frequency [Hz]	Damping (%)	Frequency [Hz]	Damping (%)	Frequency [Hz]	Damping (%)
Power	0.71	**7.3**	0.71	**3**	0.71	**9.4**	0.68	**14.2**
Current	0.71	**7.3**	0.71	**3.2**	0.7	**6.8**	0.73	**13.8**

Table 15: The damping frequency and ratio of the active power and current in Line 5-2 – 50% wind power penetration and POD only activated in WPP1.

5.6.2.2 POD only activated in WPP2

Figure 31 illustrates the impact of the POD controller on its input signals namely current magnitude or active power for the test cases TC_POD$_8$ (I&ΔQ_{POD}), TC_POD$_9$ (P&ΔP_{POD}) and TC_POD$_{10}$ (P&ΔQ_{POD}) defined in Table 6 for 50% wind penetration case with local measurement, when only POD in WPP2 is activated.

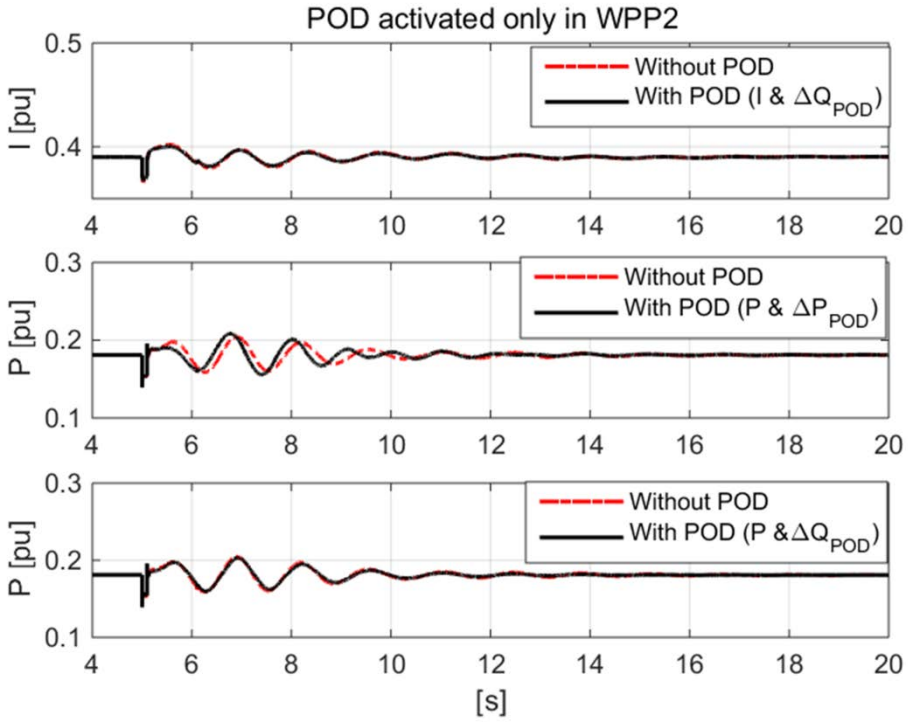

Figure 30: Input signals (current and active power in Line 7-8) of the POD controller with and without POD for TC_POD$_8$, TC_POD$_9$ and TC_POD$_{10.}$ - POD activated only in WPP2.

Based on Figure 31, the following remarks can be done on the impact of the three types of POD controller, activated only in WPP2:

- POD - I&ΔQ_{POD} and POD - P&ΔQ_{POD} do not have any damping influence on the current in Line 7-8.
- POD - P&ΔP_{POD} does have a very small damping impact on the oscillations of active power in Line 7-8

The POD controllers' input/output waveforms and the active and reactive power of WPP3, for the test cases TC_POD$_8$ (I&ΔQ_{POD}), TC_POD$_9$ (P& ΔP_{POD}) and TC_POD$_{10}$ (P&ΔQ_{POD}) defined in Table 6 for 50% wind penetration case with local measurement,

when only POD in WPP2 is activated, are illustrated in Appendix B (i.e. Figure 61 and Figure 62).

The impact on the current and active power in Line 7-8 of the POD controller, using the three input/output configurations for POD controller, i.e. POD - I&ΔQ_{POD}, POD - P& ΔP_{POD} and P&ΔQ_{POD}, is illustrated in Figure 32 and in Table 17.

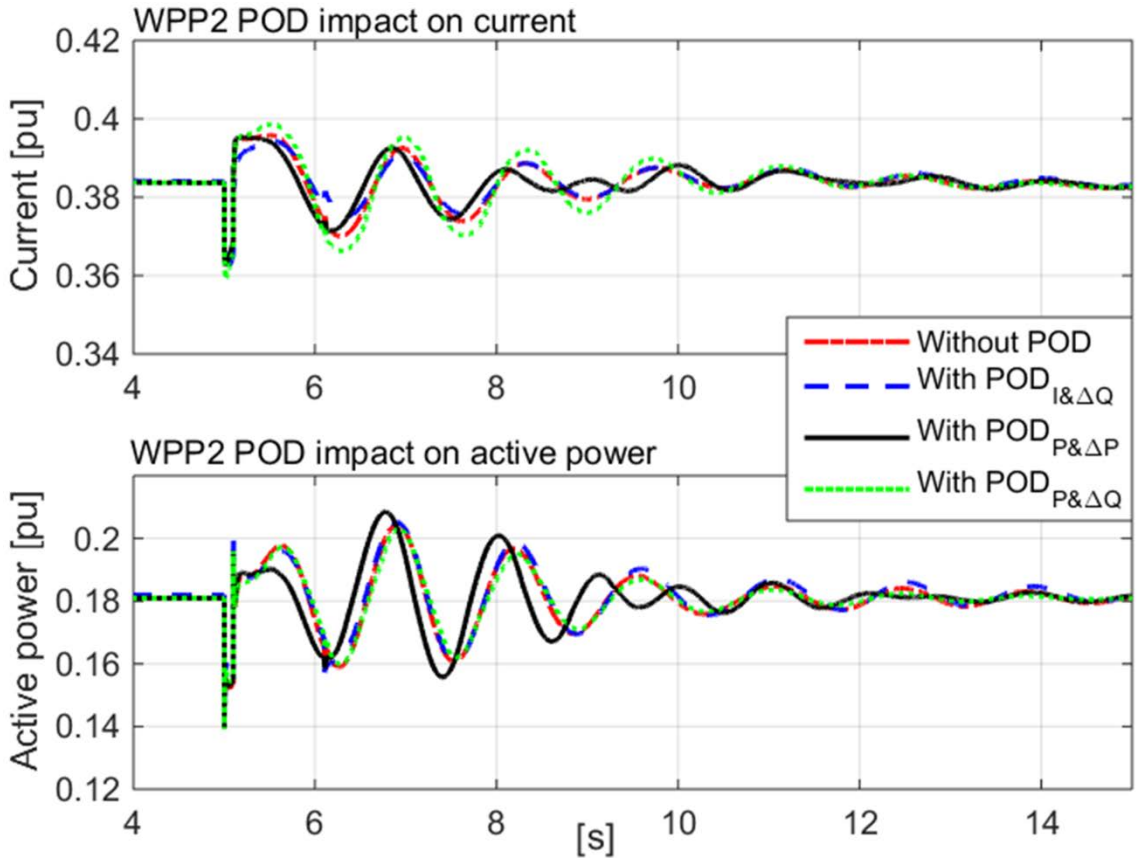

Figure 31: Impact of the three types of POD controllers(I&$\Delta Q_{POD,,}$ P&ΔQ_{POD} and P&ΔQ_{POD}) activated only in WPP1 for 50% wind power penetration on current and power measured locally in Line 7-8.

The figures in Table 17 are very well in concordance with the performance results illustrated in Figure 32. Notice that modulating reactive power with current as input signal into POD worsens the damping ratio both on current and on power. The best damping performance on both power and current is given by modulating active power with active power as input into the POD controller. The POD controller modulating reactive power with the use of active power as input has the same damping effect on power and current.

50%-WPP2	**Without POD**		**POD - I & ΔQ**		**POD - P & ΔP**		**POD - P & ΔQ**	
Signal	Frequency [Hz]	Damping (%)	Frequency [Hz]	Damping (%)	Frequency [Hz]	Damping (%)	Frequency [Hz]	Damping (%)
Power	0.71	**7.3**	0.7	**6.3**	0.73	**22.8**	0.71	**11.2**
Current	0.7	**6.4**	0.7	**5.8**	0.66	**15.4**	0.73	**11.9**

Table 16: The damping frequency and ratio of the active power and current in Line 7-8 – 50% wind power penetration and POD only activated in WPP2.

5.6.2.3 POD only activated in WPP3

Figure 33 illustrates the impact of the POD controller on its input signals namely current magnitude or active power for the test cases TC_POD$_8$ (I&ΔQ_{POD}), TC_POD$_9$ (P& ΔP_{POD}) and TC_POD$_{10}$ (P&ΔQ_{POD}) defined in Table **6** for 50% wind penetration case with local measurement, when only POD in WPP3 is activated.

Based on Figure 33, the following remarks can be done on the impact of the three types of POD controller, activated only in WPP3:

- POD - I&ΔQ_{POD} does not have any damping influence on the current in Line 4-6.
- POD - P&ΔP_{POD} does have a very small damping impact on the oscillations of active power in Line 4-6.
- POD - P&ΔQ_{POD} sligtly increases the oscillations in the active power in Line 4-6.

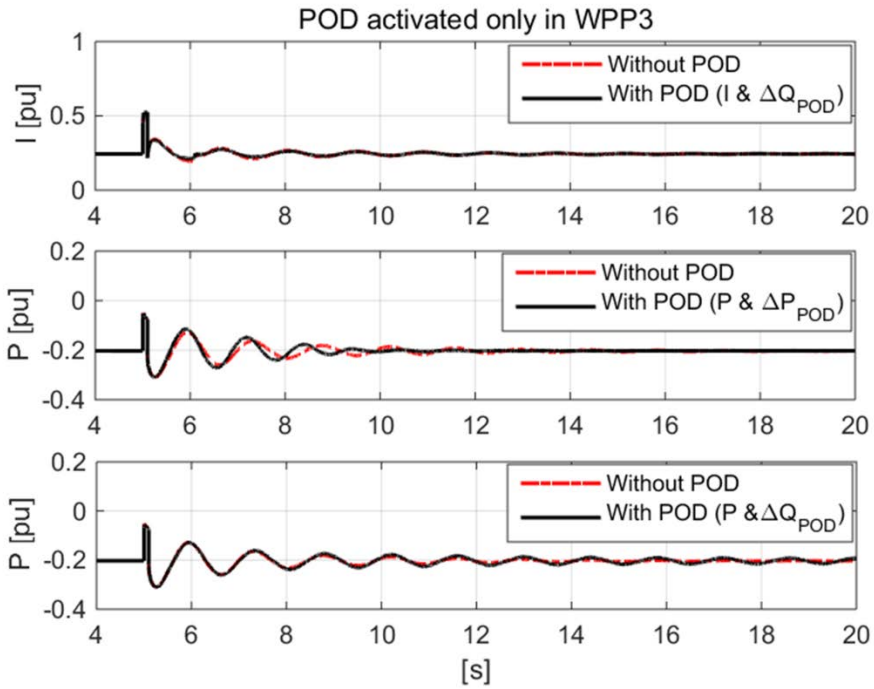

Figure 32: Input signals (current and active power in Line4-6) of the POD controller with and without POD for TC_POD$_8$, TC_POD$_9$ and TC_POD$_{10}$.- POD activated only in WPP3.

The POD controllers' input/output waveforms and the active and reactive power of WPP3, for the test cases TC_POD$_8$ (I&ΔQ_{POD}), TC_POD$_9$ (P& ΔP_{POD}) and TC_POD$_{10}$ (P&ΔQ_{POD}) defined in Table 6 for 50% wind penetration case with local measurement, when only POD in WPP3 is activated, are illustrated in Appendix B (i.e. Figure 63 and Figure 64).

The impact on the current and active power in Line 4-6 of the POD controller, using the three input/output configurations for POD controller, i.e. POD - I&ΔQ_{POD}, POD - P& ΔP_{POD} and P&ΔQ_{POD}, is illustrated in Figure 34 and in Table 18.

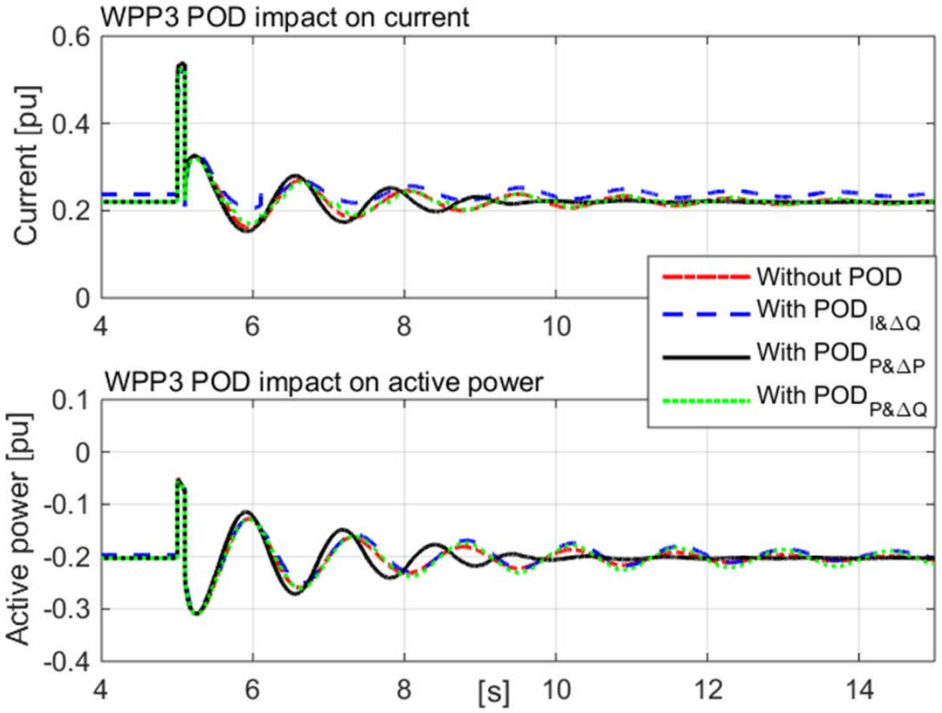

Figure 33: Impact of the three types of POD controllers (I&$\Delta Q_{POD,,}$ P&ΔQ_{POD} and P&ΔQ_{POD}) activated only in WPP3 for 50% wind power penetration on current and power measured locally in Line 4-6.

The figures in Table 18 are very well in concordance with the performance results illustrated in Figure 34. Notice that modulating reactive power with current as input signal into POD worsens the damping ratio both on current and on power. The best damping performance on both power and current is given by modulating active power with active power as input into the POD controller. The POD controller modulating reactive power with the use of active power as input worsens the damping of the power.

50%-WPP3	**Without POD**		**POD - I & ΔQ**		**POD - P & ΔP**		**POD - P & ΔQ**	
Signal	Frequency [Hz]	Damping (%)	Frequency [Hz]	Damping (%)	Frequency [Hz]	Damping (%)	Frequency [Hz]	Damping (%)
Power	0.71	**7.4**	0.71	**5.3**	0.9	**23.4**	0.71	**3.1**
Current	0.71	**7**	0.71	**4.8**	0.89	**22.4**	0.7	**7.6**

Table 17: The damping frequency and ratio of the active power and current in Line 4-6 – 50% wind power penetration and POD only activated in WPP3.

5.6.2.4 POD activated simultaneously in WPP1, WPP2 and WPP3

The simulations to investigate POD activated simultaneously in WPP1, WPP2 and WPP3, are performed under the assumption that the same input/output pair POD configuration is activated in all three WPPs.

Figure 35 illustrates the impact of the POD - I&ΔQ_{POD} controller on the current magnitude on Line 5-2, Line 7-8 and Line 4-6 respectively for 50% wind penetration case with local measurement, when POD - I&ΔQ_{POD} controller is activated in all three wind power plants: WPP1, WPP2 and WPP3.

Based on Figure 35, the following remarks can be done on the impact of the POD - I&ΔQ_{POD} controller activated in all three WPPs on the POD input signal, namely the current magnitude on Line 5-2, Line 7-8 and Line 4-6 :

- POD - I&ΔQ_{POD} activated in WPP1 does not damp the current in Line 5-2, introducing only a small change in the phase of the current.
- POD - I&ΔQ_{POD} activated in WPP2 does damp the oscillations in the current in Line 7-8,
- POD - I&ΔQ_{POD} activated in WPP3 has very small damping impact on the oscillations in the current in Line 4-6,

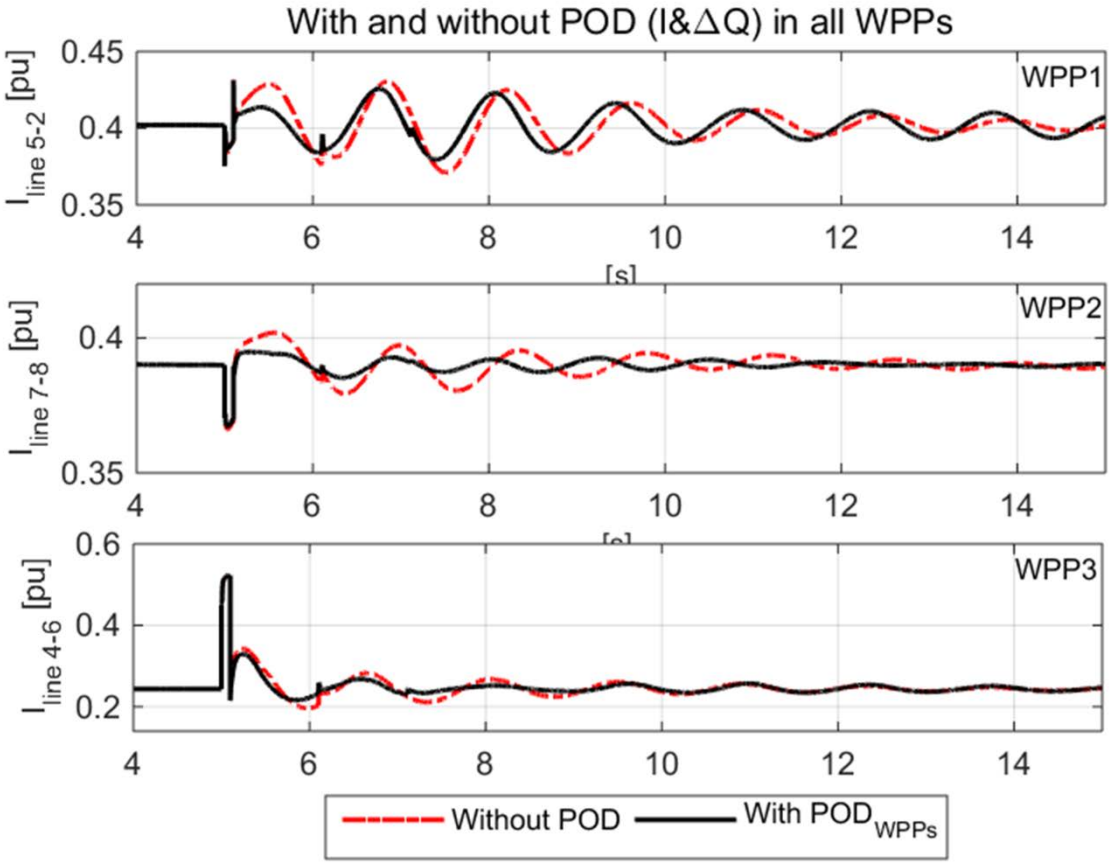

Figure 34: Input signal (current magnitude) of the POD - I&ΔQ_{POD} controller for TC_POD_8 - with POD activated in all three WPPs or not.

Figure 36 illustrates the impact of the POD - P&ΔP_{POD} controller on the active power on Line 5-2, Line 7-8 and Line 4-6 respectively for 50% wind penetration case with local measurement, when POD - P&ΔP_{POD} controller is activated in all three wind power plants: WPP1, WPP2 and WPP3.

Based on Figure 36, the following remarks can be done on the impact of the POD - P&ΔP_{POD} controller activated in all three WPPs on the POD input signal, namely the current magnitude on Line 5-2, Line 7-8 and Line 4-6:

- POD - P&ΔP_{POD} activated in WPP1 does damp the active power in Line 5-2.

- POD - $P\&\Delta P_{POD}$ activated in WPP2 does damp the oscillations in the active power in Line 7-8,
- POD - $P\&\Delta P_{POD}$ does not damp the oscillations in the active power in Line 4-6

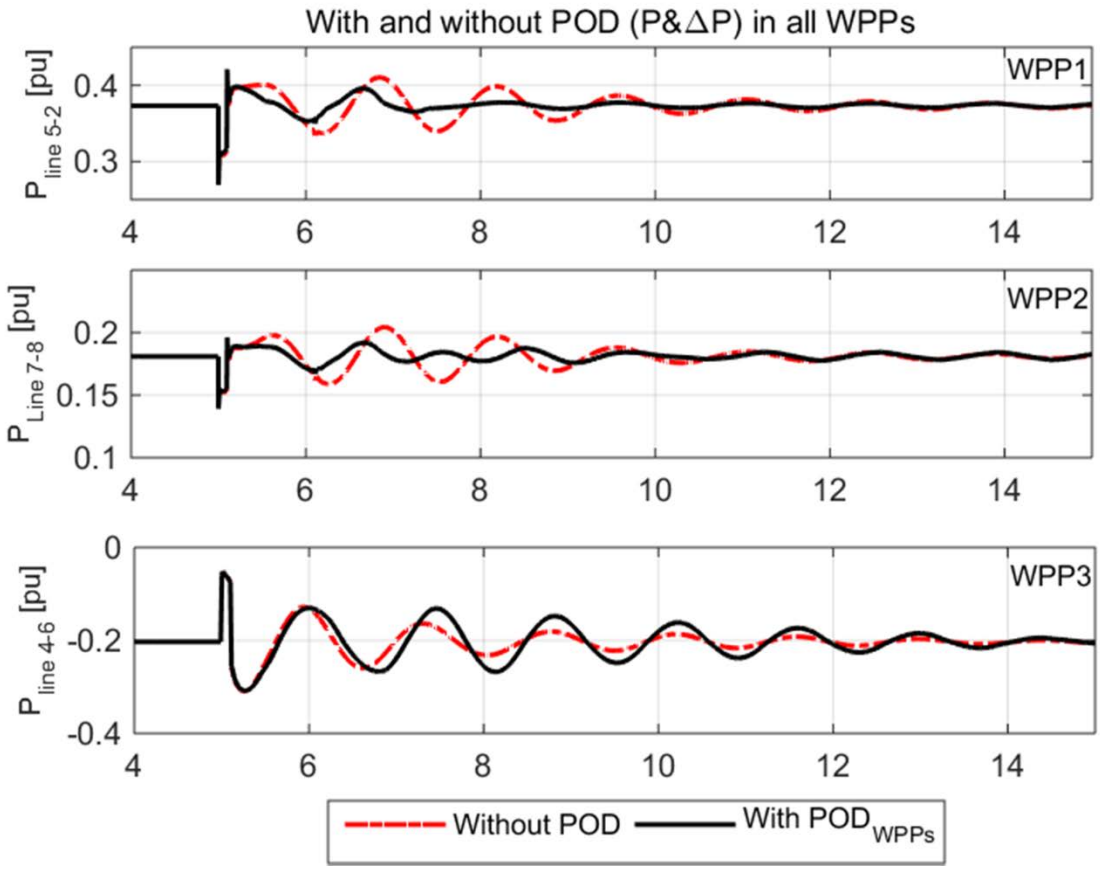

Figure 35: Input signal (active power) of the POD - $P\&\Delta P_{POD}$ controller for TC_POD_9 - with POD activated in all three WPPs or not.

Figure 37 illustrates the impact of the POD - $P\&\Delta Q_{POD}$ controller on the active power on Line 5-2, Line 7-8 and Line 4-6 respectively for 50% wind penetration case with local measurement, when POD - $P\&\Delta Q_{POD}$ controller is activated in all three wind power plants: WPP1, WPP2 and WPP3.

Based on Figure 37, the following remarks can be done on the impact of the POD - $P\&\Delta Q_{POD}$ controller activated in all three WPPs on the POD input signal, namely the current magnitude on Line 5-2 , Line 7-8 and Line 4-6

- POD - $P\&\Delta Q_{POD}$ activated in WPP1 does damp the active power in Line 5-2.
- POD - $P\&\Delta Q_{POD}$ activated in WPP2 does slightly damp the oscillations in the active power in Line 7-8.
- POD - $P\&\Delta Q_{POD}$ activated in WPP3 does not damp the active power in Line 4-6, also introducing a small change in the phase of the current.

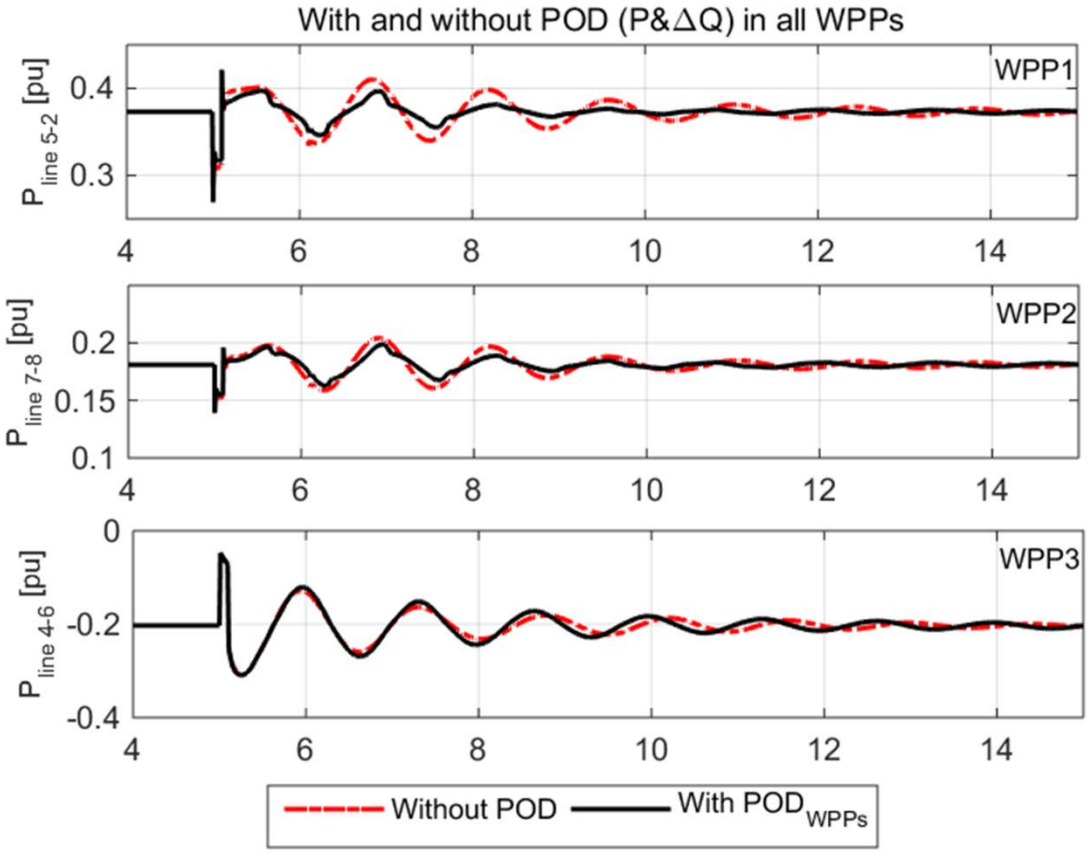

Figure 36: Input signal (active power) of the POD - P&ΔQ$_{POD}$ controller for TC_POD$_{10}$ - with POD activated in all three WPPs or not.

The impact of the each input/output pair configuration of POD controller (I&ΔQ$_{POD}$, P&ΔP$_{POD}$ and P&ΔQ$_{POD}$), on the current and active power measured locally in Line 5-2 in the 50% wind power penetration is illustrated in Figure 38.

Based on Figure 38, the following remarks

- The current in Line 5-2 is best damped when in all three WPPs the POD - P&ΔP$_{POD}$ is activated.
- The active power in Line 5-2 is best damped when in all three WPPs the POD - P&ΔP$_{POD}$ is activated. Almost the same damping performance is also obtained when in all three WPPs the POD - P&ΔQ$_{POD}$ is activated. The POD - I&ΔQ$_{POD}$ amplifies the oscillations instead of damping them.

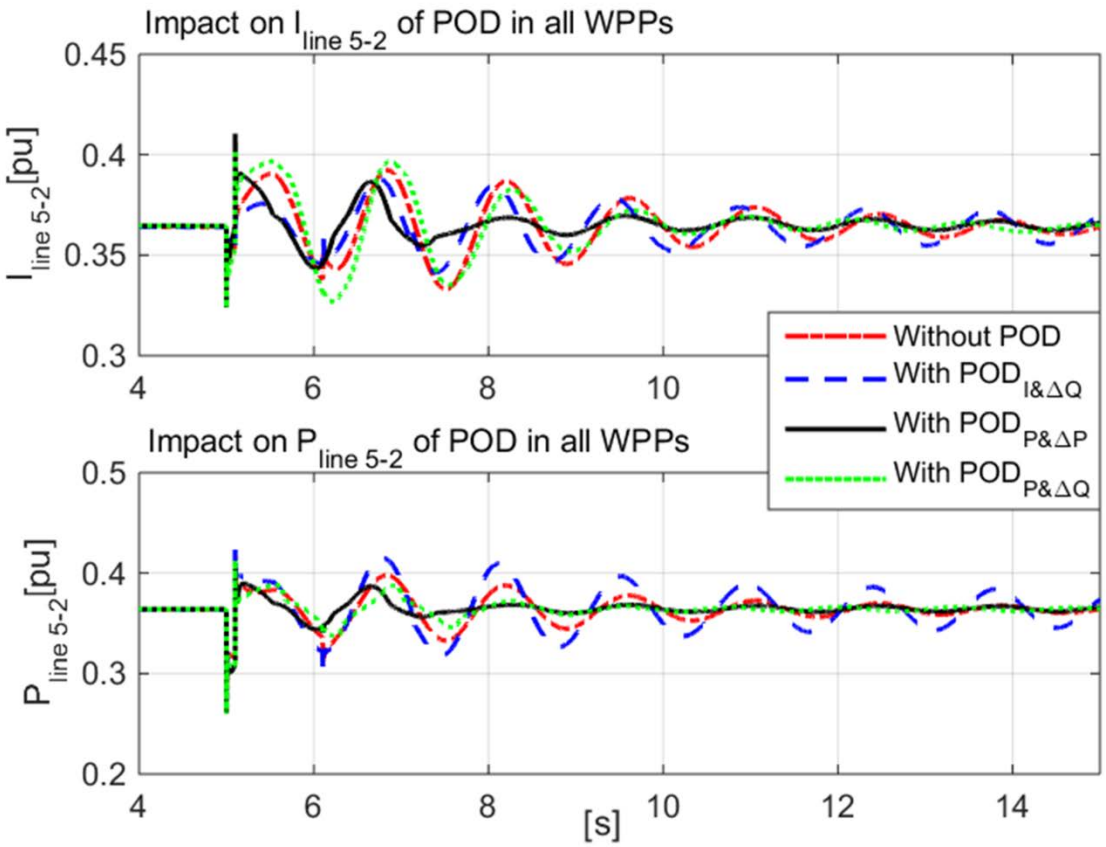

Figure 37: Impact of each type of POD controller (I&$\Delta Q_{POD,}$ P&ΔQ_{POD} and P&ΔQ_{POD}), the same type being activated in all WPPs, for 50% wind power penetration on current and power measured locally in Line 5-2.

The impact of the input/output pair configuration of POD controller (I&ΔQ_{POD}, P&ΔP_{POD} and P&ΔQ_{POD}), on the current and active power measured locally in Line 7-8 in the 50% wind power penetration is illustrated in Figure 39. Similar remarks as those for Figure 38 can be done for Figure 39, namely that the POD – P&ΔP_{POD} controller, activated in all three WPPs, namely with active power as input signal (measured locally) and ΔP_{POD} as output signal, has the best damping performance both on the current and the active power measured in Line 7-8.

The impact of the input/output pair configuration of POD controller (I&ΔQ_{POD}, P&ΔP_{POD} and P&ΔQ_{POD}), on the current and active power measured locally in Line 4-6 in the 50% wind power penetration is illustrated in **Figure 40**. Notice that this time the POD – P&ΔP_{POD} controller worsens the oscillations, while the other two types of POD controller almost do not have any impact on the oscillations.

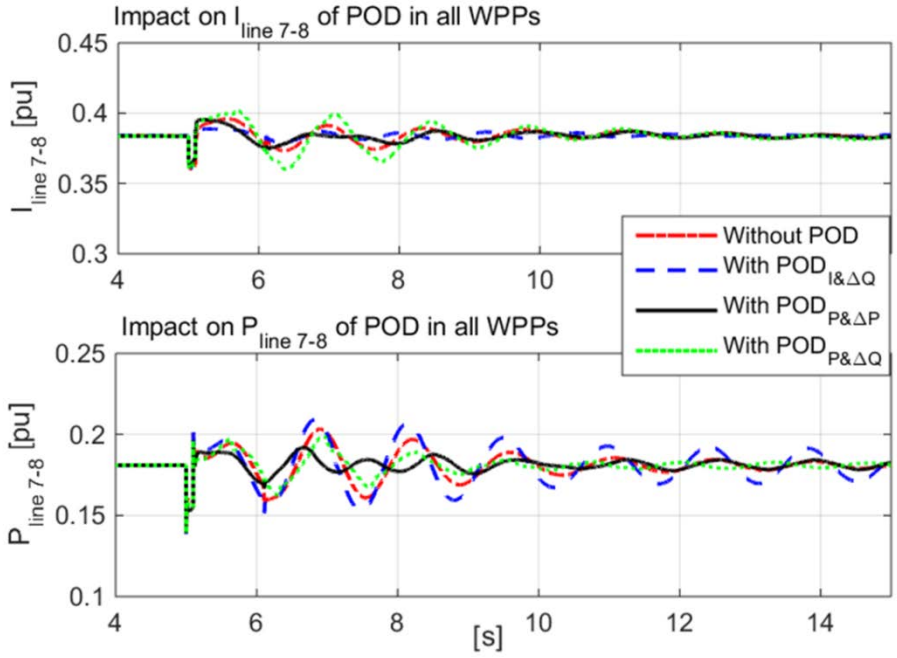

Figure 38: Impact of each type of POD controller ($I\&\Delta Q_{POD,}$ $P\&\Delta Q_{POD}$ and $P\&\Delta Q_{POD}$), the same type being activated in all WPPs, for 50% wind power penetration on current and power measured locally in Line 7-8.

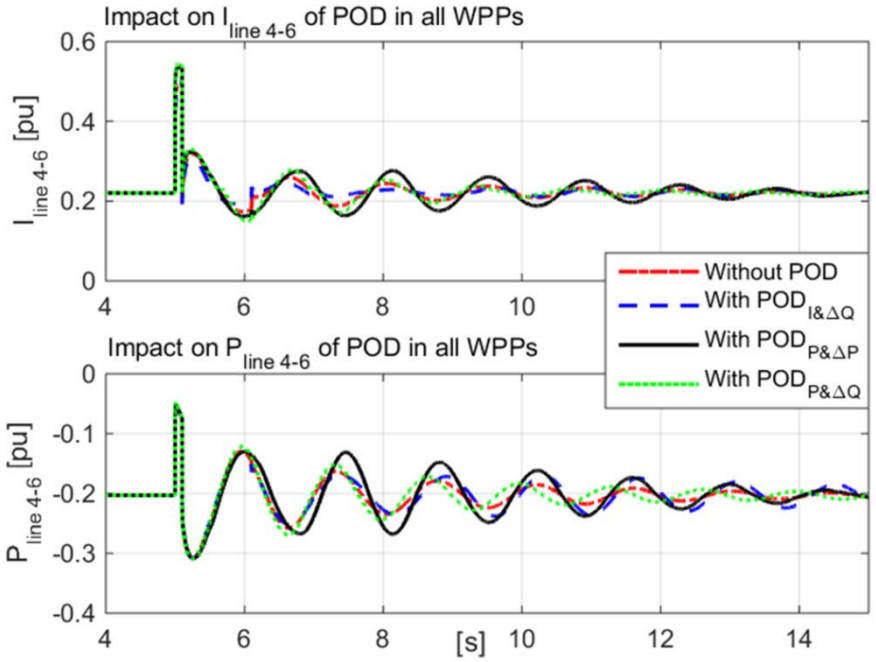

Figure 39: Impact of each type of POD controller ($I\&\Delta Q_{POD,}$ $P\&\Delta Q_{POD}$ and $P\&\Delta Q_{POD}$), the same type being activated in all WPPs, for 50% wind power penetration on current and power measured locally in Line 4-6.

In addition to the conclusions stated above, the simulation results are summarized in for the impact of POD on current and active power signals, respectively.

	Line	Without POD		With POD from	POD - I & ΔQ		POD - P & ΔP		POD - P & ΔQ	
		Frequency [Hz]	Damping (%)		Frequency [Hz]	Damping (%)	Frequency [Hz]	Damping (%)	Frequency [Hz]	Damping (%)
Current	5 - 2	0.71	**7.30**	**WPP1 only**	0.71	**3.20**	0.70	**6.80**	0.73	**13.80**
	7 - 8	0.70	**6.40**	**WPP2 only**	0.70	**5.80**	0.66	**15.40**	0.73	**11.90**
	4 - 6	0.71	**7.00**	**WPP3 only**	0.71	**4.80**	0.89	**22.40**	0.70	**7.60**
	5 - 2	0.70	**6.90**	**WPP1, WPP2, WPP3**	0.70	**3.40**	0.72	**3.20**	0.75	**13.70**
	7 - 8	0.70	**6.20**	**WPP1, WPP2, WPP3**	0.69	**14.50**	0.73	**8.80**	0.72	**8.90**
	4 - 6	0.70	**6.40**	**WPP1, WPP2, WPP3**	0.71	**1.30**	0.72	**5.60**	0.75	**9.50**
	Line	Without POD		With POD from	POD - I & ΔQ		POD - P & ΔP		POD - P & ΔQ	
		Frequency [Hz]	Damping (%)		Frequency [Hz]	Damping (%)	Frequency [Hz]	Damping (%)	Frequency [Hz]	Damping (%)
Power	5 - 2	0.71	**7.30**	**WPP1 only**	0.71	**3.00**	0.71	**9.40**	0.68	**14.20**
	7 - 8	0.71	**7.30**	**WPP2 only**	0.70	**6.30**	0.73	**22.80**	0.71	**11.20**
	4 - 6	0.71	**7.40**	**WPP3 only**	0.71	**5.30**	0.90	**23.40**	0.71	**3.10**
	5 - 2	0.70	**6.80**	**WPP1, WPP2, WPP3**	0.71	**3.00**	0.72	**1.70**	0.77	**7.80**
	7 - 8	0.70	**6.90**	**WPP1, WPP2, WPP3**	0.71	**2.70**	0.75	**2.60**	0.78	**9.20**
	4 - 6	0.70	**6.90**	**WPP1, WPP2, WPP3**	0.71	**2.60**	0.72	**5.60**	0.76	**6.70**

Table 18: Summarize of POD with local measurement for 50% wind power penetration test case.

Based on the assumptions defined for the present test cases for the studied generic power system model, the following general remarks can be done when local measurements are used as inputs in POD controllers:

- The POD – I & ΔQ_{POD} controller worsens the damping ratio both for power and current. There is only one exception, namely the current at Line 7- 8 is damped by this configuration, when it is applied in all WPPs.
- When the POD controller is active in only one turbine – the POD P & ΔP_{POD} has the best damping performance on both current and power, followed by the POD – P & ΔQ_{POD} controller.
- In general the individual activation of POD (i.e. only in one WPP) has better damping performance than the case when all WPPs have activated the POD controller. Due to the activation of the PODs at the same time with same parameters without considering the location of the WPP and input/output combination of the POD, the power oscillation can be worsen compared to the each individual activation of POD in WPPs.
- The POD P & ΔQ_{POD} seems to be the best POD configuration when the POD is activated in all WPPs, though its damping effect is not significant.
- A coordinated tuning of the POD controller for each WPP might be necessary to reduce the burden of each WPP. This fact might be difficult to implement in practice, as the WPPs might have different owners. In conventional power plants the PSSs (power system stabilizers) are also tuned considering the other PSSs' parameters for inter-area oscillations in a power system. The difference and advantages using WPP POD functionality are that both the active and the reactive power references can be adjusted faster than conventional WPPs with respect to different inputs (local or remote measurement points). Since the conventional power plants are the source of the problem for the power system oscillation, WPPs can support their PSS capabilities as an attractive solution.

- Voltage variations at the PCC buses for POD – I & ΔQ_{POD} and POD P & ΔQ_{POD} are within the acceptable limits (±5%)

6 Synchronizing Power (SP)

SP is an embedded feature of synchronous generators, which reduces the load angle between groups of SC in the PS. If the load angle becomes too high, the SGs lose torque and system becomes unstable. An increase in the share of converter connected generators, as the case of WPPs, decreases the amount of the available SP in the system. As result, it may be necessary to introduce SP as a new AS product. The idea of SP from WPP, is thus to improve the steady state stability of the PS by giving additional power into the system from the WPP, in cases when the rotor angle rises above a safe limit. Typically the change in rotor angle is determined by a load change. Based on the rotor or voltage angle deviation the SP controller increases the active power output of the WPP and thus compensate with active power the lack of SP in the system.

6.1 SP controller

This control functionality attempts to improve the steady-state stability of the power system by giving an additional power in-feed into the system from the WPP, in cases when the voltage or rotor angle rises above a limit value deemed as safe by pre-run load flow studies. Typically the change in power angle is determined by a demand change [3].

In the present investigation, the SP controller has two possible input signals, namely rotor angle difference between 2 generators and the voltage angle difference between 2 busbars. The output of the controller is the delta active power ΔP_{SP} that has to be summed up with the overall active power reference provided by the WPPC [1].

6.2 Definition of simulation test cases for SP

In order to analyse the impact of the proposed control on the steady-state synchronising power, the system load in Bus 3 is ramped up-down **75%,** as illustrated in Figure **43**. The ramp change has duration of 5 seconds each and it represents slow increase load events in the power system. The tests are done with the aggregated WPP model and the wind speed is assumed 10m/s and 10% reserve is allocated.

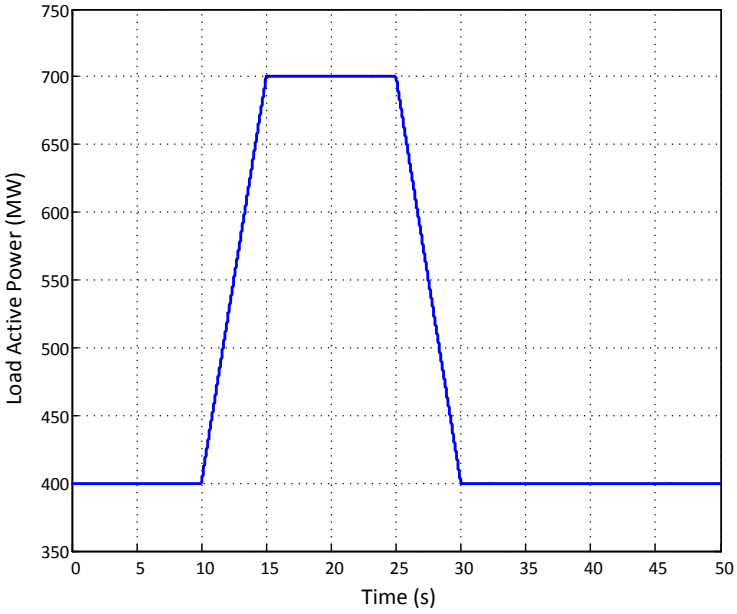

Figure 40: Load change – ramped up-down 75%.

The simulation test cases for SP are indicated in Table 22.

PoM	Input signal	Output signal	% wind	Ctrl. Parameters	Case SP no.	
Base Case	-	-	30%	SP-P1	TC_SP_0	0
Bus 2 & Bus 3	Rotor angle $\Delta\delta_{23}$	ΔP_{SP}	30%	SP-P1	TC_SP_1	1
	Voltage angle $\Delta\theta_{23}$	ΔP_{SP}	30%	SP-P1	TC_SP_2	2
Bus 2 & Bus 4	Voltage angle $\Delta\theta_{24}$	ΔP_{SP}	30%	SP-P1	TC_SP_3	3
Bus 2 & Bus 5	Voltage angle $\Delta\theta_{25}$	ΔP_{SP}	30%	SP-P1	TC_SP_4	4

Table 19: Simulation test cases for SP.

6.3 Success criteria

The effectiveness of SP functionality has to be evaluated based on the criteria defined in Table 23.

Characterization	Specifications	Identifier
Voltage angles	Differences in voltage and load angles should remain below 30 degrees in all cases.	IR-SC-01

Table 20: Success criteria for SP

6.4 Simulation results of the SP test cases

In order to present the impact of the SP controller on the power system, the rotor angle difference between the Generator 2 (connected to Bus 10 at Figure 4) and the Generator 3 (connected to Bus 11 at Figure 4) is given in Figure 44. The base case (30% wind penetration) without the SP control action from WPPs has the highest deviation value and also the case TC_SP_4 is the same situation due to inactivation of the SP controller with the angle deviation between the Bus 2 and Bus 5. The bus angle differences for the last three cases are given in Figure 45. In Figure 45 the angle differences are used for the SP controller as inputs.

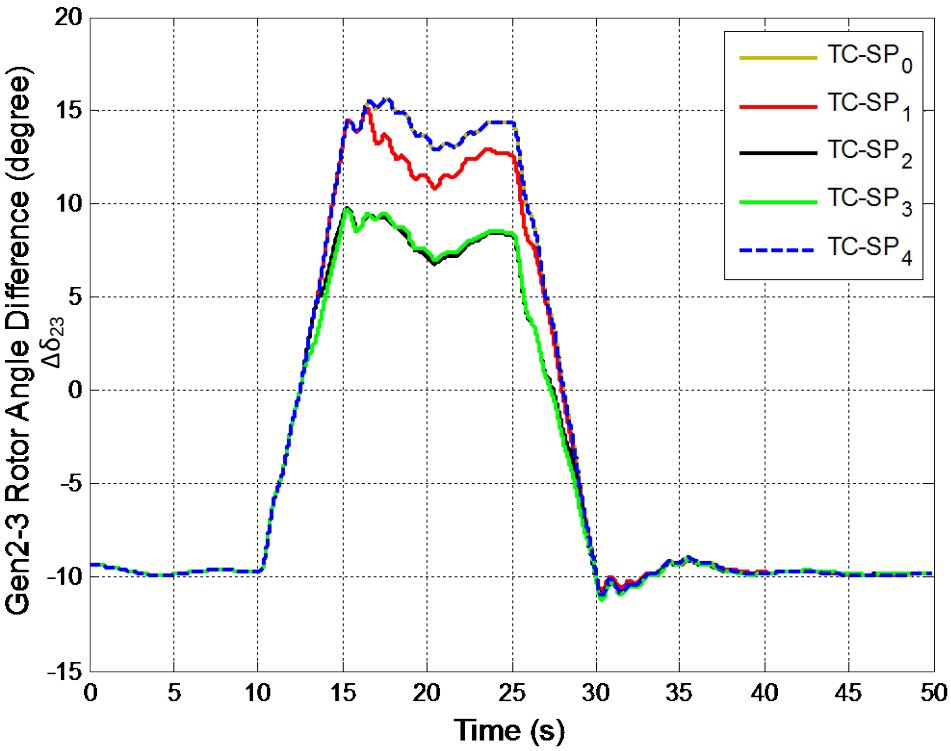

Figure 41: Impact of the SP controller on rotor angle difference between Gen2 and Gen3

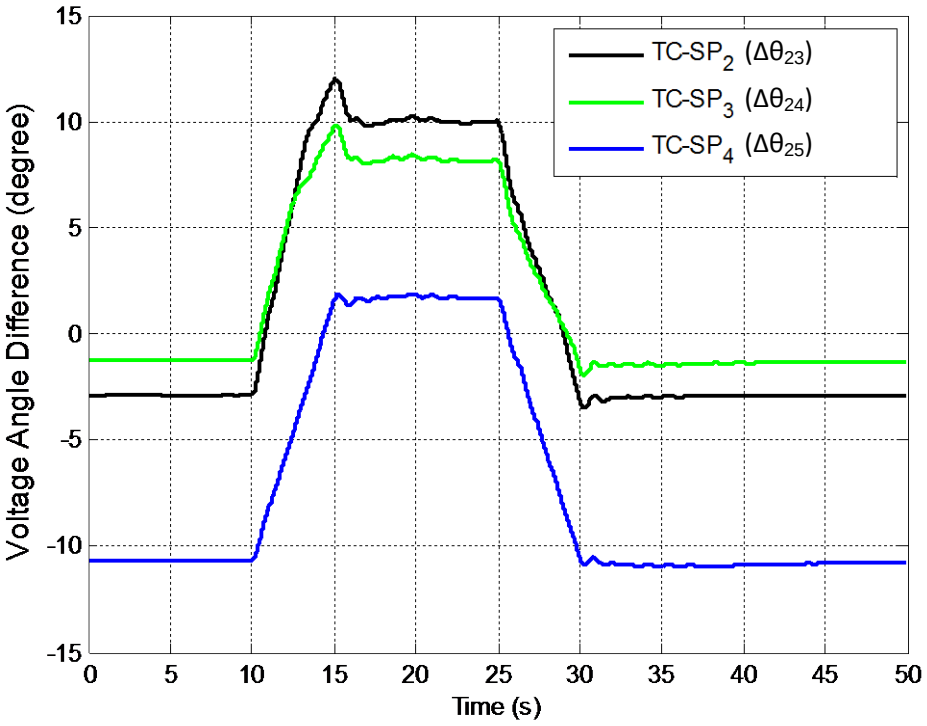

Figure 42: Impact of the SP controller on voltage angle difference between the buses (black:Bus2-Bus3, green:Bus2-Bus4, blue:Bus2-Bus5).

As it can be seen from the SP controller impact on the rotor angle difference (Figure 44), the active power increase of the WPPs due to angle increase can help to decrease the angle separation between generators and also the buses. Accordingly, the impact of the SP controller on the wind turbine dynamics is presented in Figure 46. The SP controller parameters are kept same for all the cases (as in Table 22), and with these parameters in the first case (TC_SP_1) the contributions is less due to the input where the absolute value of the angle difference is decreasing at the beginning and later at 14s the angle difference is increasing above the pre-disturbance value. Another important remark is for the last case (TC_SP_4) the angle difference is decreased during the load increase event, thus the SP controller is not activated. From the simulation results, one conclusion is that the selection of the buses for the input of the SP controller is important. Due to the location of the buses and the load flow, the angle differences can be decreased and the required performance cannot be obtained from the WPPs.

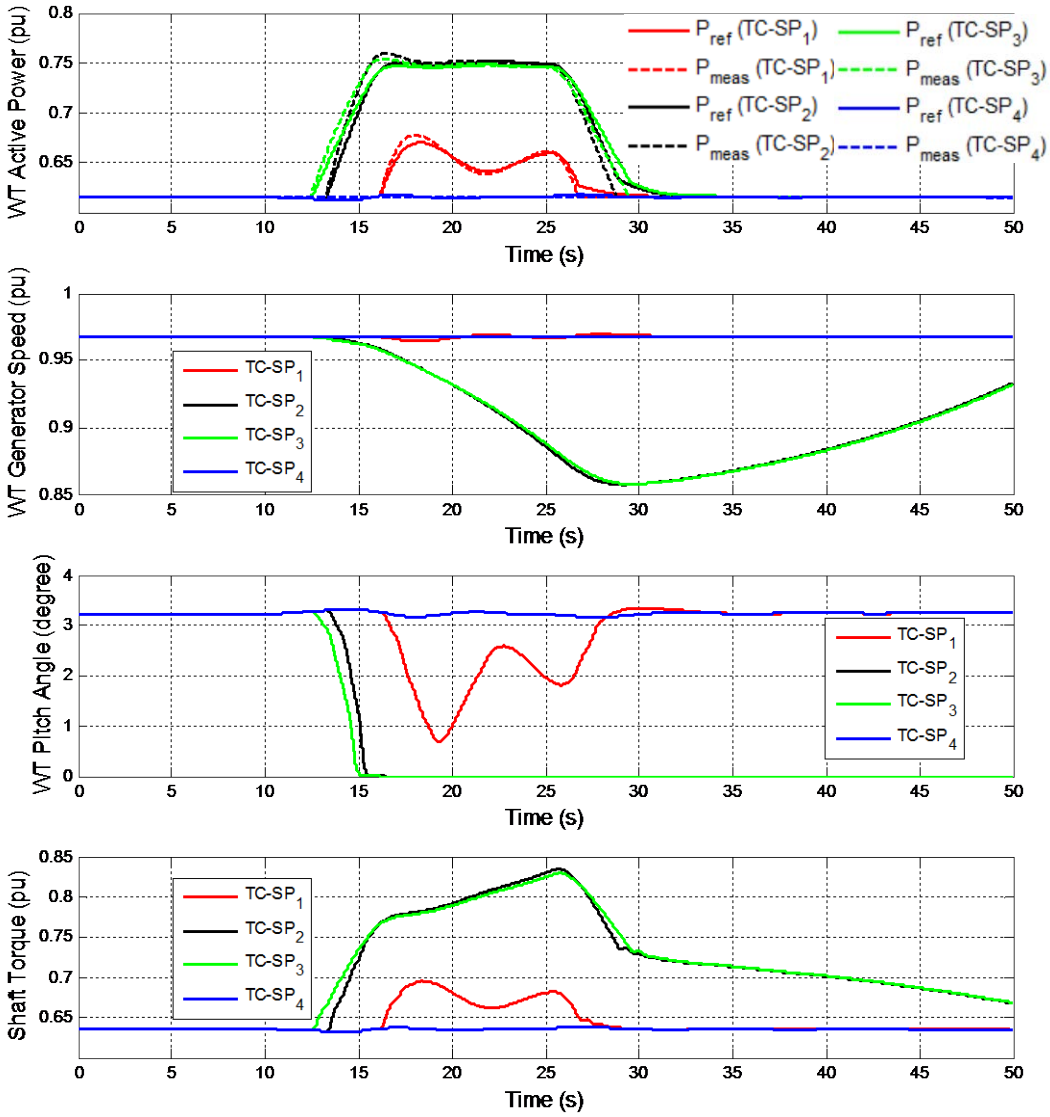

Figure 43: Wind turbine dynamics for the cases in Table 22.

When the rotor angle difference input ($\Delta\delta_{23}$) is used in the case TC_SP$_1$, the active power is oscillating according to the rotor oscillation of the Gen2 and Gen3. This oscillation mode cannot be seen in the bus voltage angle differences, and also because of the filter implementation in the SP controller (Figure 42).

If the SP controller response is investigated further, for the TC_SP$_2$ and TC_SP$_3$ cases the wind turbine is overloaded for 14 sec with 10% overloading with respect the available power (0.68 pu). This can be realized in Figure 47 and the impact of this overloading on the generator speed and shaft torque is given in Figure 47. The speed deviation is not exceeding 15% of the rated value and it is not triggering the protection.

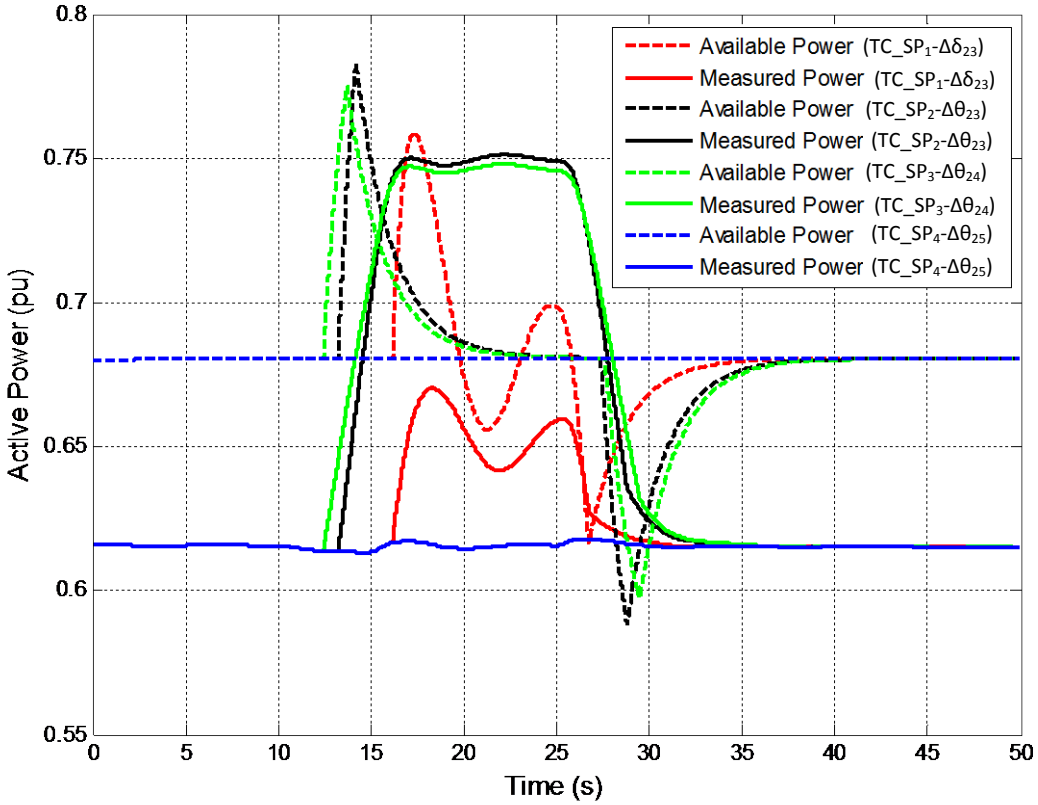

Figure 44: Wind turbine available and measured power for the cases in Table 22.

Finally, the contributions from IR controller and SP controller are presented in Figure 48. As expected the IR controller is dependent on the load change and thus the frequency deviation and acts similar to the SP controller response after the load increase. However, the POD controller is taking the active power flow as an input and the oscillations can be seen at the output of the controller. In this case (or similar cases) the POD parameters can be revised such as tuning filter parameters considering oscillations caused by specific load changes. The allocation of each controller should be carefully considered and activated not to spoil the other controllers' responses. According to these and previous results, the allocation of the enhanced ancillary services should be studied further.

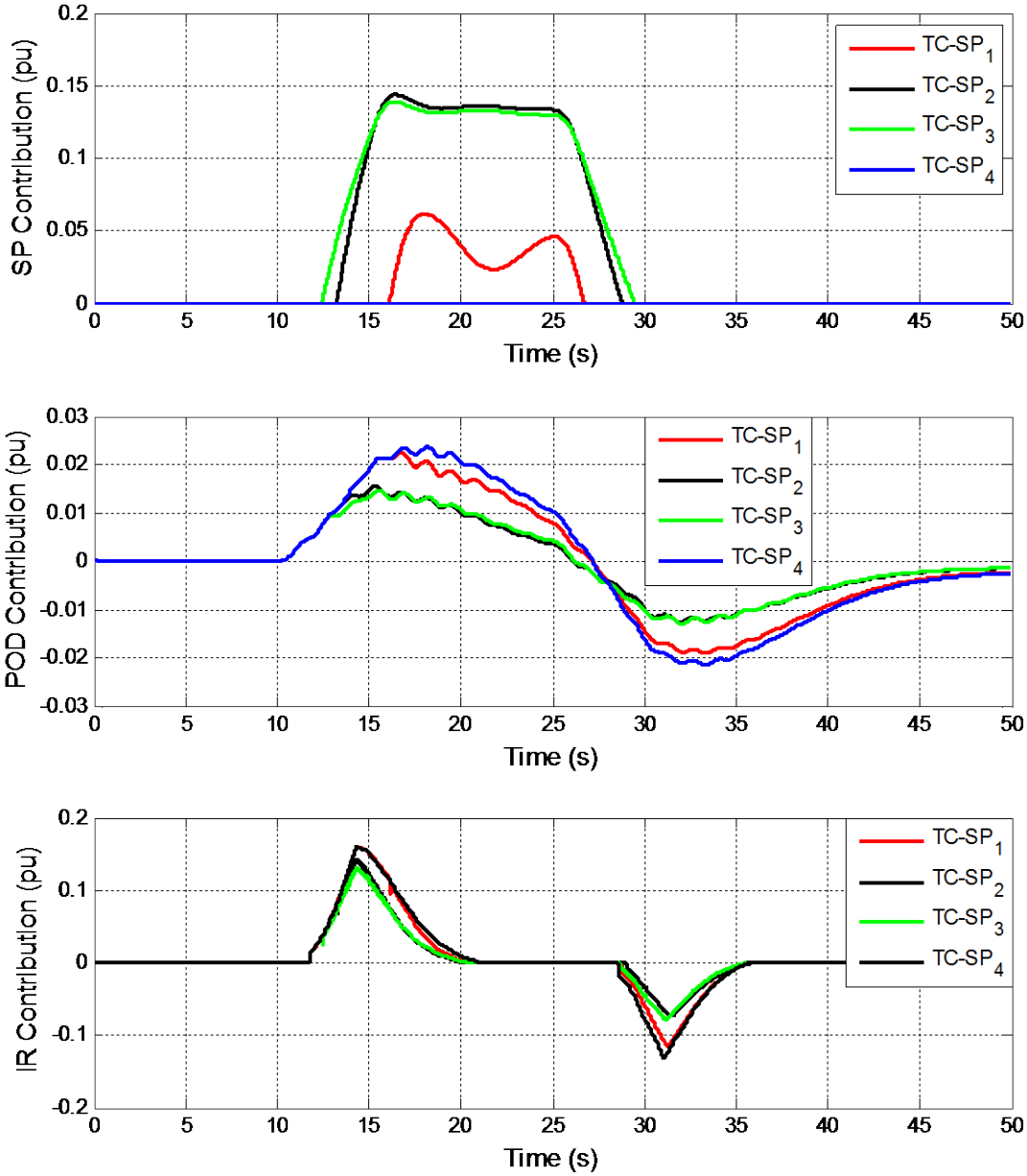

Figure 45: Advanced ancillary services' contributions for the cases in Table 22.

7 Summary

The impact of new wind power advanced ancillary services, like inertial response (IR), power oscillation damping (POD) and synchronising power (SP) on the power system has been investigated and presented in the present report.

The simulation test cases have been designed for reproducing the respective ancillary service with a realistic behaviour and operation of an island power system with various wind power penetration scenarios. The dynamics of the wind turbine and wind power plant models are suitable for positive sequence fundamental frequency (RMS) simulations. The results of the simulation test cases have shown the WPPs can support the power system stability regarding frequency, small signal and rotor angle stability. The tuning of the controller parameters is very important to sustain these stability issues in large power systems during contingency events.

The IR control functionality satisfies the predefined operational metric considering the frequency nadir, ROCOF and the double frequency dip. A 10% active power reserve in WPPs utilised for IR control is sufficient to support the grid within the wind turbine's capabilities. The size of active power reserve, the IR controller parameters and frequency disturbance event (the loss of the largest generating unit) are important in the design of a robust IR control. **Another important remark is that the calculation of ROCOF is difficult even in the simulations and can cause wrong triggering of the IR control**. In the RMS simulations, frequency is obtained from synchronous machines through an angle calculation algorithm (such as PLL or zero-crossing). Therefore the calculation of the frequency and ROCOF of the grid in RMS simulations is not including the transient dynamics existing in practice, which can influence the performance of the IR control. A complete dynamic model of the WPP and the WT is required for the IR control studies. Another future investigation can be that a coordination of the IR control between WPPs can support frequency stability of the system not to cause second frequency dip.

WPPs can contribute with POD control functionality. However the tuning of the POD control parameters is very important and dependent on the input/output pair combinations and the input measurement location (remote or local). In addition, if multiple WPPs are required to provide POD at the same time, a coordinated POD parameter tuning between WPPs (by TSOs) is crucial for the small signal stability of the power system even with the conventional power plants' PSSs.

The SP control functionality can be provided by WPPs for the steady state rotor angle stability. In the simulations the operational metrics are satisfied. However without SP controller the voltage and rotor angle differences are not exceeding the predefined operational metrics, i.e. 30 deg. Further investigations are required considering different power system models in order to present the effectiveness of the SP controller in critical scenarios close to stability limit. In these investigations, the tuning and the impact of the SP controller can be highlighted depending on the power system parameters and operating conditions.

The objectives of the report are achieved within the scope and limitations. It has been shown that WPPs can WPPs **can provide** enhanced **ancillary services** – emulating synchronous generator (inertia/fast frequency response, synchronising power and power oscillating damping). However, much work still remains to be done, particularly in the developing algorithms for service allocation, control parameter tuning, robust and adaptive control strategies, service coordination and selection for optimal input/output pair for the controllers.

More work is needed to get answers to questions addressing different aspects, as following:

- **Services allocation :**
    - is it appropriate to run in parallel with multiple functionalities?
    - which service should be prioritised?
    - can it contribute to the overall success criteria of meeting the power system needs for stabilising features?
    - can it minimise the needed reserve power allocation from wind (curtailment)?
- **Parameters tuning**
    - how is this implemented in practice for different power system scenarios?
- **Service algorithm**
    - how to select the input/output pair for POD control, for a given network?
- **Service coordination**
    - should all WPPs provide services?
    - which WPP is most suitable to provide a specific service ?

Appendix A – POD remote measurements
50% wind power penetration

A1 – POD only in WPP1

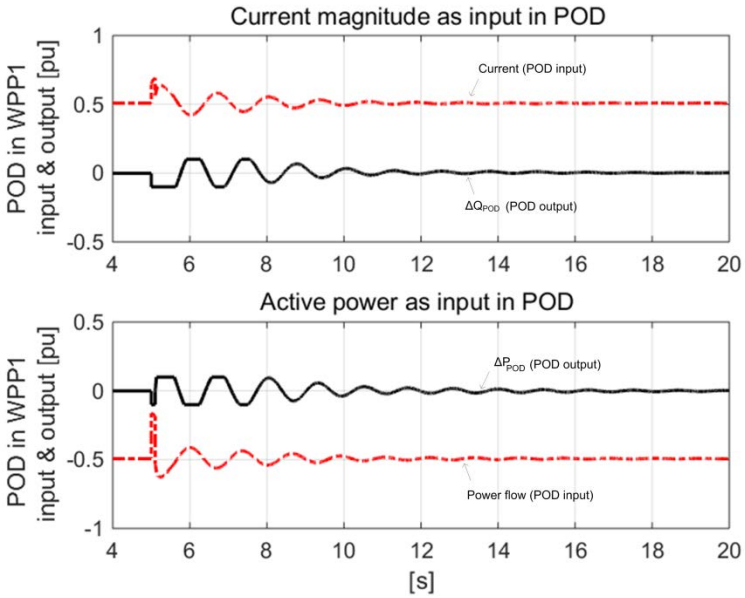

Figure 46: Waveforms of input and output of the POD controller activated in WPP1 for TC_POD_3 and TC_POD_4. Current and active power measured in Line 6-1.

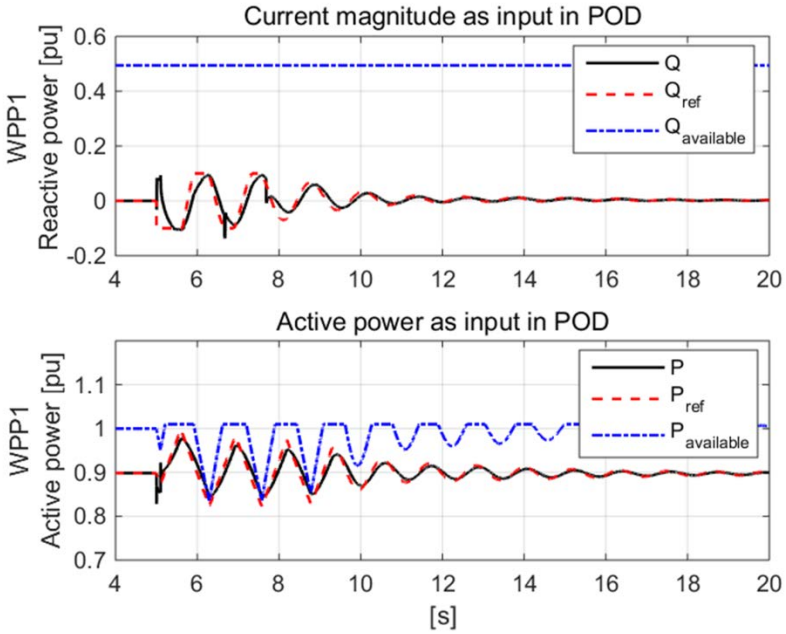

Figure 47: Active and reactive power of WPP1 in TC_POD_3 and TC_POD_4 when POD controller activated in WPP1: measurement, reference and available.

A2- POD only in WPP2

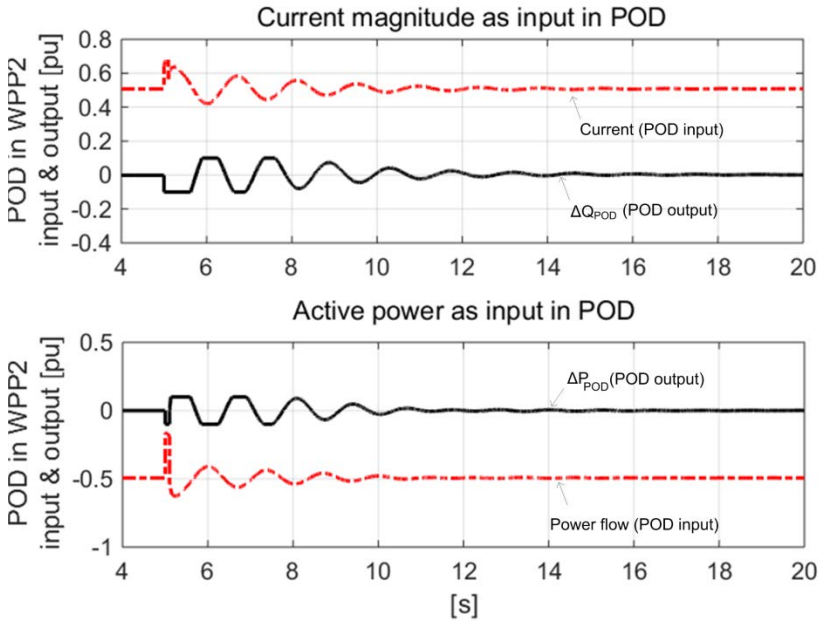

Figure 48: Waveforms of input and output of the POD controller activated in WPP2 for TC_POD_3 and TC_POD_4. Current and active power measured in Line 6-1.

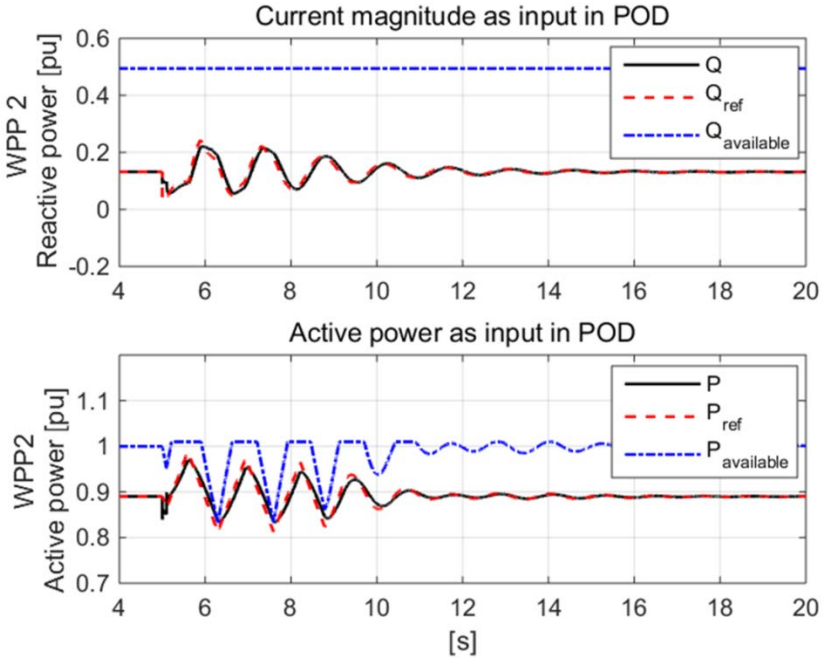

Figure 49: Active and reactive power of WPP2 in TC_POD_3 and TC_POD_4 when POD controller activated in WPP2: measurement, reference and available.

A3 - POD only in WPP3

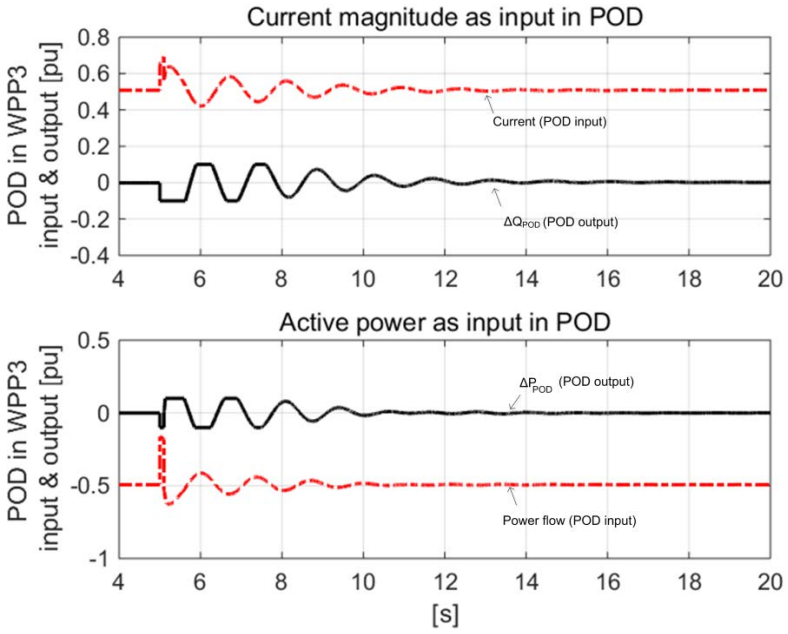

Figure 50: Waveforms of input and output of the POD controller activated in WPP3 for TC_POD_3 and TC_POD_4. Current and active power measured in Line 6-1.

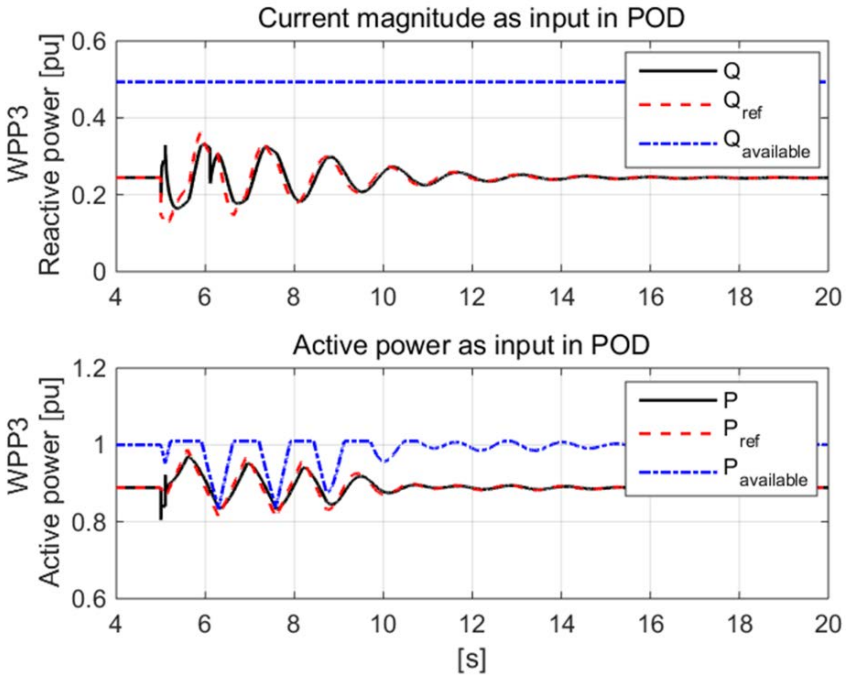

Figure 51: Active and reactive power of WPP2 in TC_POD_3 and TC_POD_4 when POD controller activated in WPP3: measurement, reference and available.

A4 – POD activated in WPP1, WPP2 and WPP3

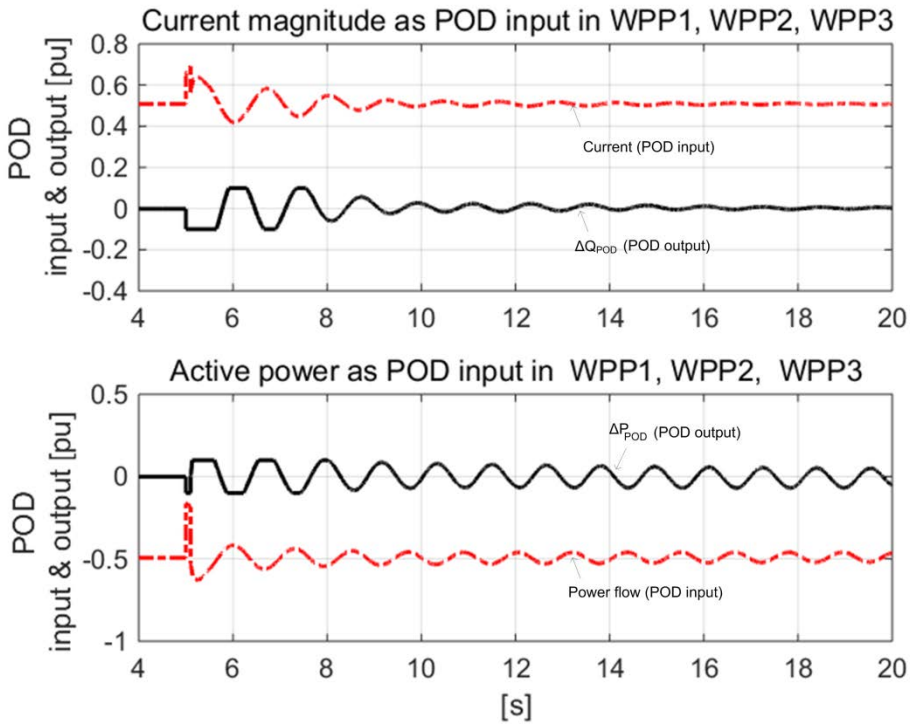

Figure 52: Waveforms of input and output of the POD controller activated in WPP1, WPP2 and WPP3 forTC_POD3 and TC_POD4. Current and active power measured in Line 6-1.

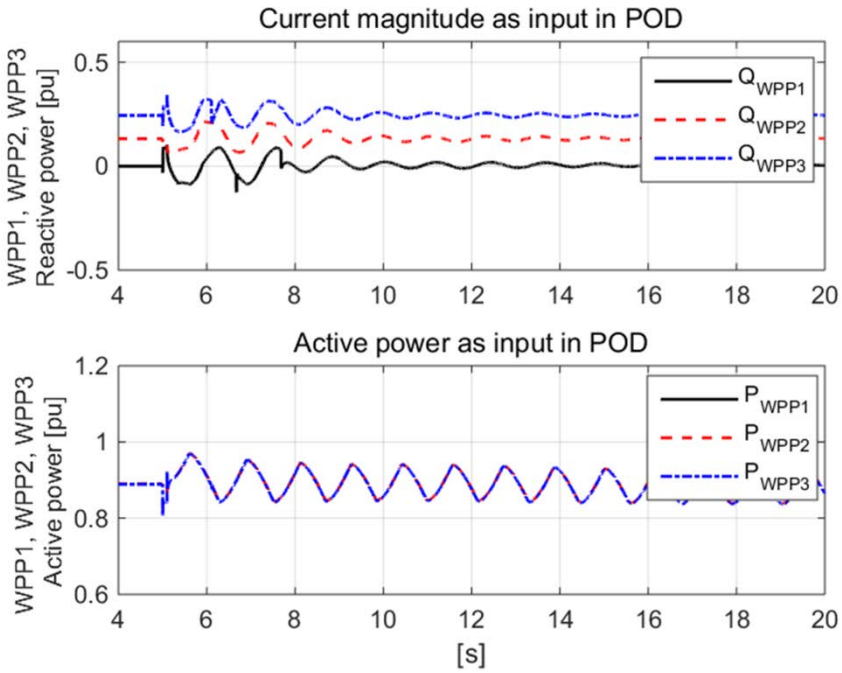

Figure 53: Active and reactive power of WPP2 in TC_POD_3 and TC_POD_4 when POD controller activated in in WPP1, WPP2 and WPP3: measurement, reference and available.

Appendix B – POD local measurements

B1 - 20% wind power penetration

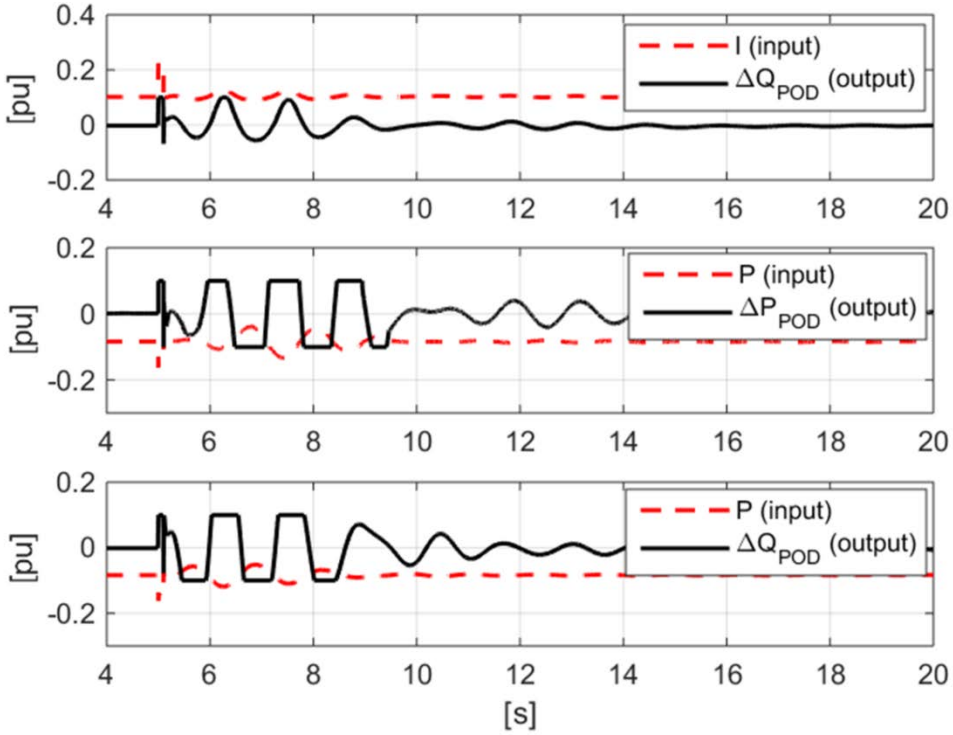

Figure 54: Waveforms of input and output of the POD controller activated in WPP1 for TC_POD_5, TC_POD_6 and TC_POD_7. Current and active power measured in Line 6-1.

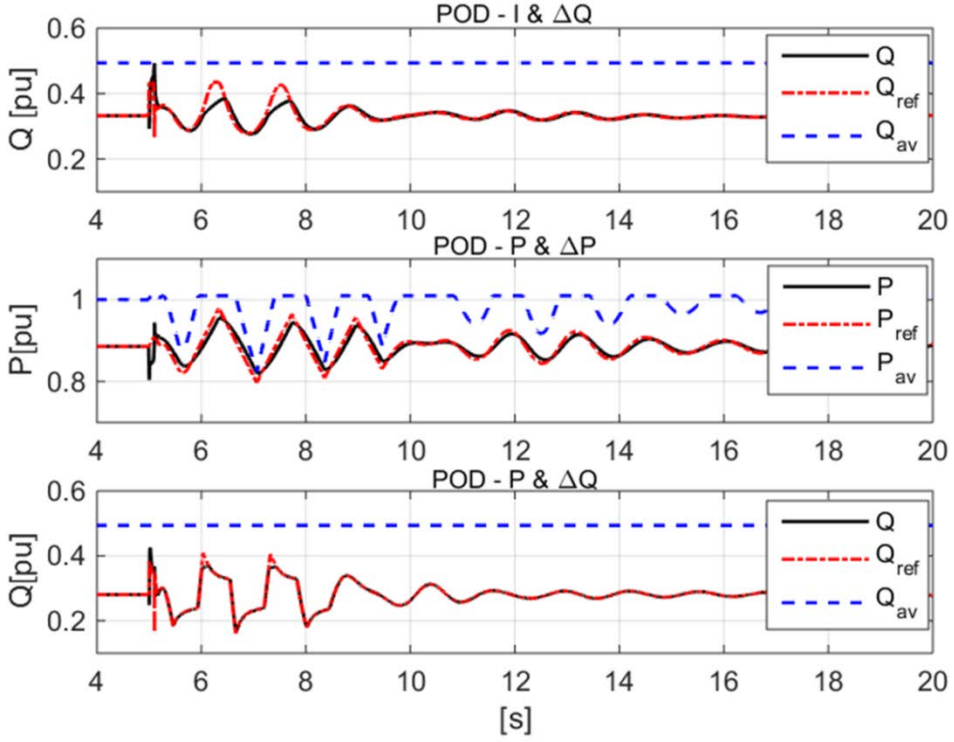

Figure 55: Active and reactive power of WPP1 in TC_POD_5 ($I\&\Delta Q_{POD}$), TC_POD_6 ($P\&\ \Delta P_{POD}$) and TC_POD_7 ($P\&\Delta Q_{POD}$) when POD controller is activated in WPP1: measurement, reference and available.

B2 – 50% wind power penetration

B2.1 – POD only in WPP1

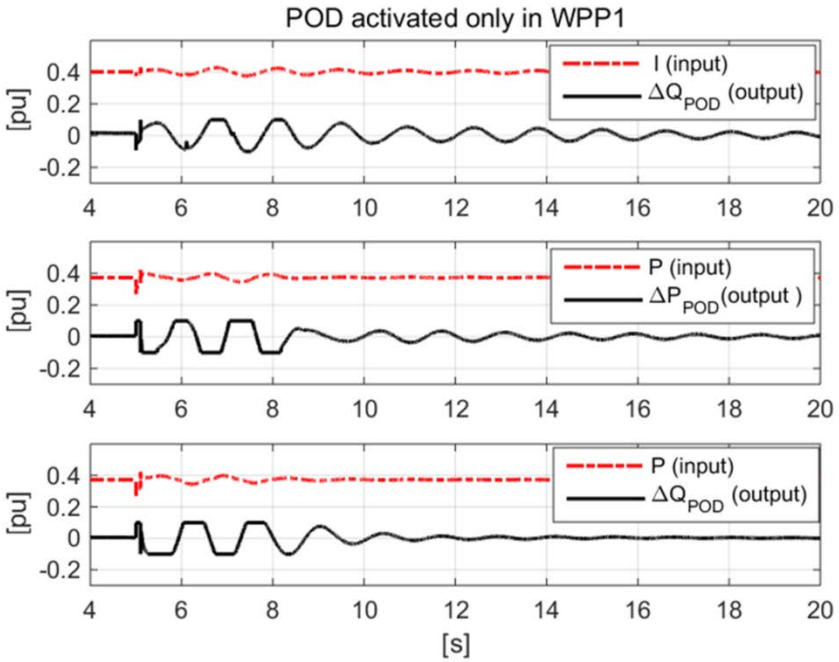

Figure 56: Waveforms of input and output of the POD controller activated in WPP1 for TC_POD_8, TC_POD_9 and TC_POD_{10}. Current and active power measured in Line 6-1.

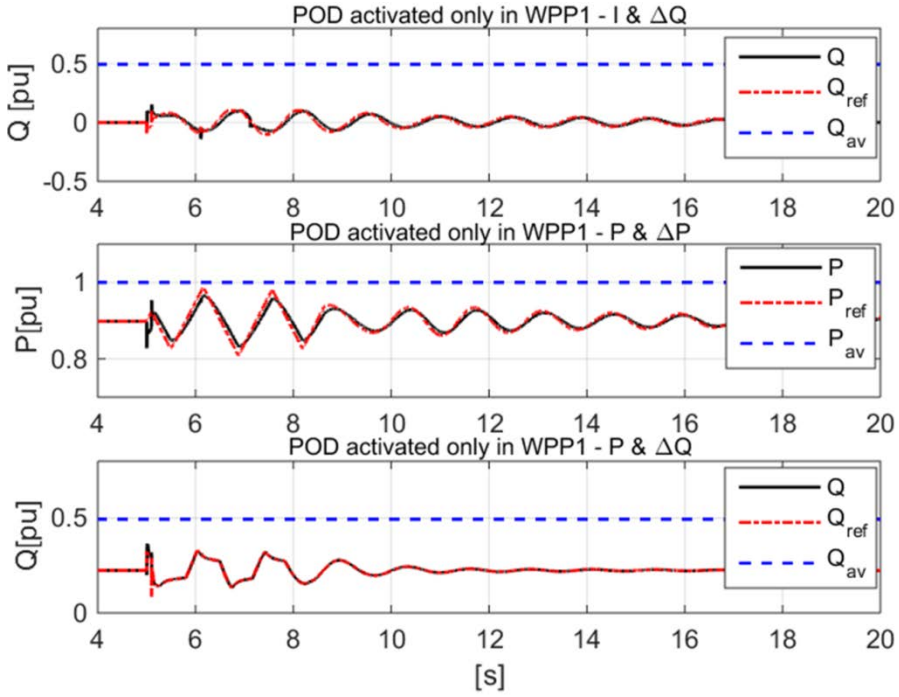

Figure 57: Active and reactive power of WPP1 in TC_POD_8, TC_POD_9 and TC_POD_{10} when POD controller is only activated in WPP1: measurement, reference and available.

B2.2 – POD only in WPP2

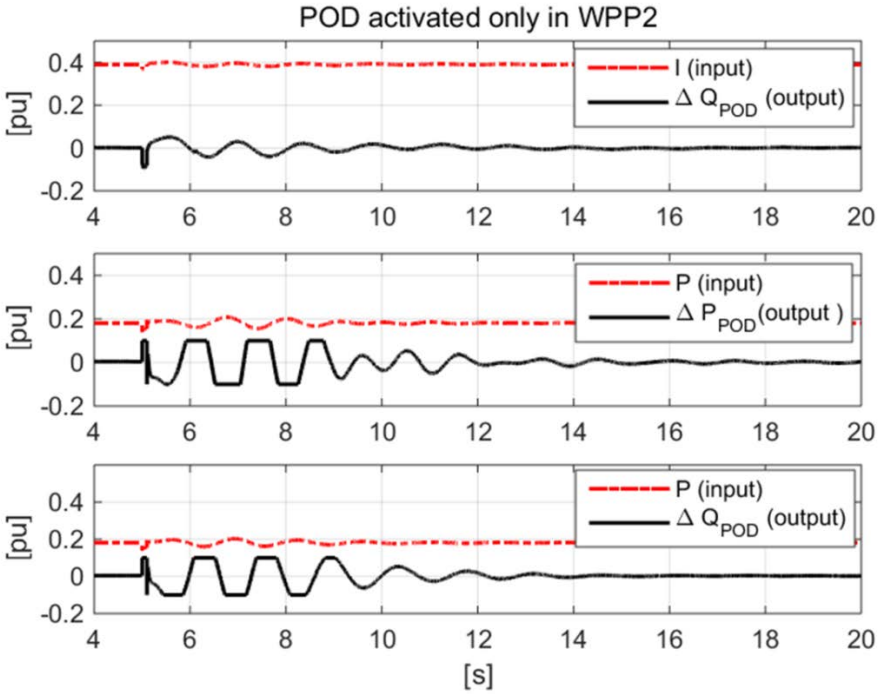

Figure 58: Waveforms of input and output of the POD controller activated in WPP2 for TC_POD_8, TC_POD_9 and TC_POD_{10}. Current and active power measured in Line 7-8.

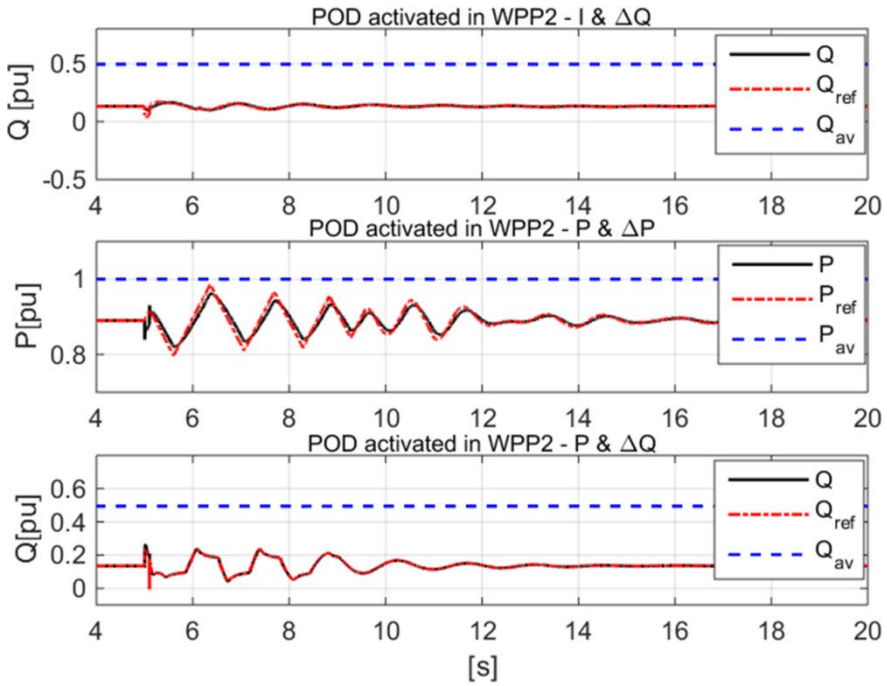

Figure 59: Active and reactive power of WPP2 in TC_POD_8, TC_POD_9 and TC_POD_{10} when POD controller is only activated in WPP2: measurement, reference and available.

B2.3 – POD only in WPP3

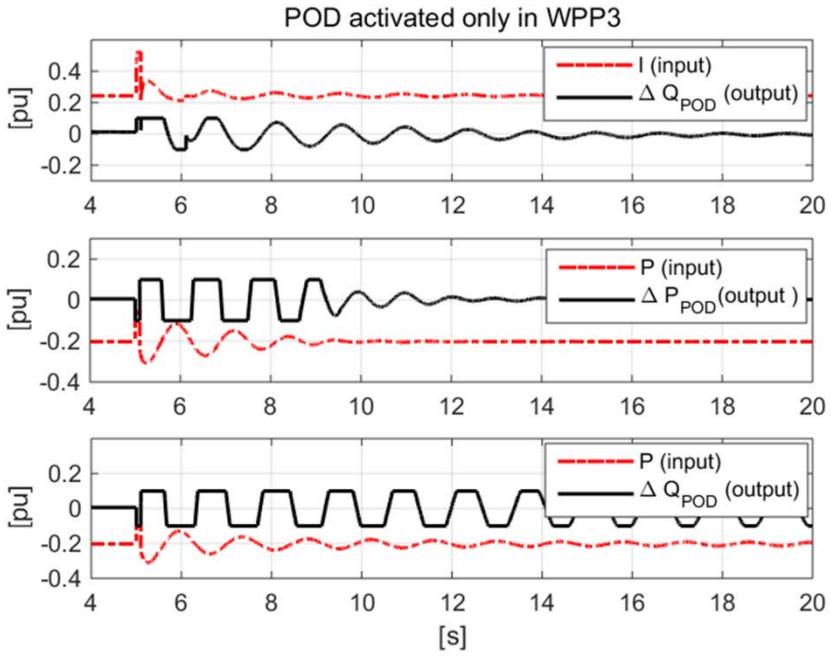

Figure 60: Waveforms of input and output of the POD controller activated in WPP3 for TC_POD_8, TC_POD_9 and TC_POD_{10}. Current and active power measured in Line 4-6.

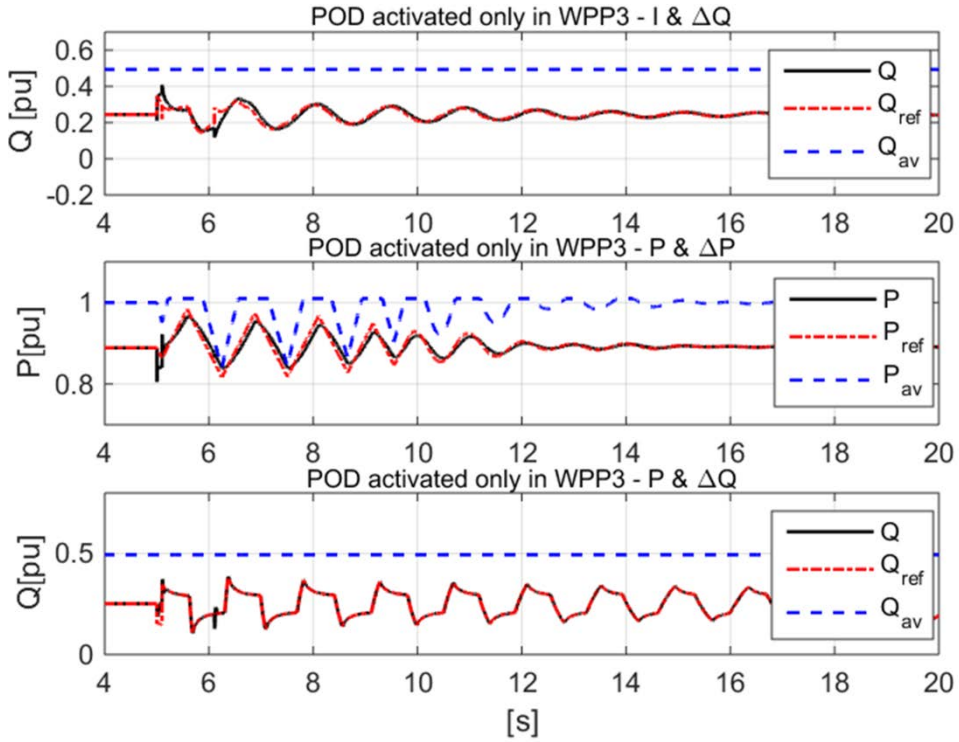

Figure 61: Active and reactive power of WPP2 in TC_POD_8, TC_POD_9 and TC_POD_{10} when POD controller is only activated in WPP3: measurement, reference and available.